# Novel Algorithm to Differentiate Astigmatism from Keratoconus

*A Dissertation submitted in partial fulfilment of the requirements for the award of degree of*

**Master of Engineering**
**in**
**Electronic Instrumentation and Control**

**Submitted By**

**SARAH ALI HASAN**
Roll No: 801251019

**Under the Guidance of**
**Dr. MD SINGH**
Assistant Professor

**Department of Electrical and Instrumentation Engineering**
**Thapar University**
(Established under the section 3 of UGC act, 1956)
Patiala, 147004, Punjab, India
July 2014

# DECLARATION

I hereby certify that the work is being presented in this thesis work entitled "**Novel algorithm to differentiate Astigmatism from Keratoconus**" in partial fulfilment of award of degree of Master of Engineering in Electronics Instrumentation & Control submitted in Electrical & Instrumentation Engineering Department, Thapar University, Patiala is an authentic record of my own work carried under the supervision of **Dr. MD Singh**, Assistant Professor, Department Of Electrical & Instrumentation Engineering, Thapar University, Patiala, Punjab.

Date: 18-07-2014

Sarah Ali Hasan
801251019

I certify that the above statement made by the student is correct to the best of my knowledge and belief.

Date: 18.07.14

**(Dr. MD Singh)**
Assistant Professor,
EIED,Thapar University

Countersigned By

**( Dr.Ravinder Agarwal )**
Head Of Department
Department of Electrical &
Instrumentation Engineering
Thapar University, Patiala.
Punjab

**( Dr. S.K. Mohapatra )**
Dean of Academic Affair
Thapar University,Patiala
Punjab

(Dr. Amod Kumar)
Acting Director,
Central Scientific Instruments Organisation
Chandigarh - 160030



ii

# ACKNOWLEDGMENT

I would like to express my gratitude **to Dr. Prakash Gopalan,** Director of Thapar University, Patiala, to **Dr.Ravinder Agarwal**, Head of the Department of Electrical & Instrumentation Engineering, Thapar University, Patiala and to **Dr. MD Singh**, my guide, Professor, Electrical & Instrumentation Department, Thapar University Patiala.

My deep thanking to Dr. Randhawa (Randhawa Eye Hospital, Patiala) for their kind help, and providing me with the necessary images and diagnosis data by Dr.Randhawa himself.

I raise my gratefulness to Allah the almighty "who taught me by the pen" for guiding me and giving me strength to finish this work especially and for all his graces upon me during my scientific and general life. This gratefulness is accessible to my parents, the second reason of my existence, for their endless love and encouragement to me always.

My deep thanks to all my teachers starting from primary school and ending with masters, for their unlimited support and guidance. A special thanks once more to my guide for his encouragement, stimulated suggestions and help. Also my thanks to all my family members, friends and colleagues who helped me making this work feasible.

Last but not least; my special thanks to students, researchers or scholars who may make the next step developing this work and enhance the literature or the practical medical applications with contributions that helps making this world a better place for all human kind.

Place: Thapar University Sarah Ali Hasan
Date:

# ABSTRACT

Astigmatism is a very common eye disorder. The cornea of the normal eye has a uniform curvature, with resulting equal refracting power over its entire surface. Light rays refracted by this cornea are not brought to a single point focus, and retinal images from objects both distant and near are blurred and may appear broadened or elongated. This refractive error is called astigmatism. Keratoconus is an ecstatic dystrophy characterized by progressive thinning, steepening, and apical conic protrusion of the cornea. Keratoconus can cause substantial distortion of vision, with multiple images, streaking and sensitivity to light. Symptoms are similar in both of the two diseases that make it difficult even for experienced ophthalmologists to make a decision on some cases whether they are keratoconic or only astigmatic eyes. Diagnosis of these visual disorders has been developed vastly in the last two decades. The existing methods are either diagnosing astigmatism or keratoconus separately or classify those using different techniques. The proposed algorithm is novel and simple method for diagnosing astigmatism and keratoconus and classifying them by combining the latest topographic facilities along with image processing techniques. One of the most popular topographic and pachemetry machines is PENTACAM, due to its high precision and quality of Pentacam images (colour coded maps), the unharmed technology, ease of use and availability. Physicians interpret the colour coded images to diagnose & treat patients with eye refracting issues manually. In the proposed work, an attempt has been made to make this process computerized by means of image processing techniques.

# TABLE OF CONTENTS

# LIST OF FIGURES

# LIST OF TABLES

# CHAPTER 1
# INTRODUCTION

## 1.1 Overview

Normal vision and the ability to communicate with world visually; is a grace that human kind always try to maintain at the best condition along the history. Within the two previous centuries vast range of evolutions took place in engineering and medicine side by side which gave the human kind better qualified and quantified life, and development still in progress and no doubt in Ophthalmology.

Corneal topography plays an important role in the management of patients undergoing refractive surgery. It is therefore vital for any eye care professionals involved in this field to have a good understanding of its principles and applications. Which make it a big responsibility on instrumentation engineers to provide the up-to date analysis and developments to the corneal topography industry, educational purposes as well as manufacturers and developers.

## 1.2 Structure of an eye & process of vision

The human eye is the organ which gives us the sense of sight. It allows us to see and recognize the figures, colors, and dimensions of objects in the world by processing the light they reflect or emit. This organ is able to detect a range of frequencies varies from dim to bright light, but it cannot sense an object when light is absent. Light here means the electromagnetic radiation. A typical human eye can see wavelengths from about 380 to 750 nm & about 790 to 400 terahertz. Figure (1) shows the position of visible light on the electromagnetic spectrum.

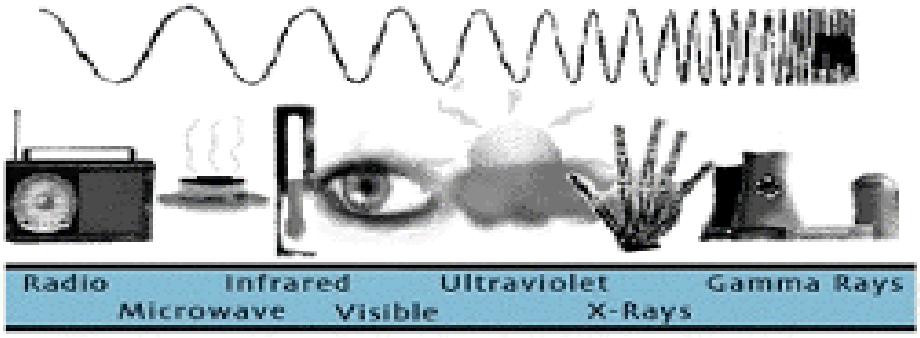


Figure 1 visible light on the electromagnetic spectrum [1]

Presence of two eyes allows making our sight stereoscopic (i.e.; to form the 3D image). The right retinal side of each eye transfers through an optic nerve "the right part" of image in the right part of a brain, and similarly for the left retinal side. Then two parts of the image right and left - connects together by the brain. As each eye perceives the "own" picture, the infringement of joint movement of the right and left eyes can break binocular sight. Simply speaking, you will see simultaneously two absolutely different pictures.

## 1.3 Anatomy of human eye

The eye can be named the difficult optical device. Its primary aim is "to transfer" the right image to an optic nerve. The basic functions of an eye**:**

- The optical system projecting the image;
- The system perceiving and "coding" the received information for a brain;
- A "serving" life-support system.

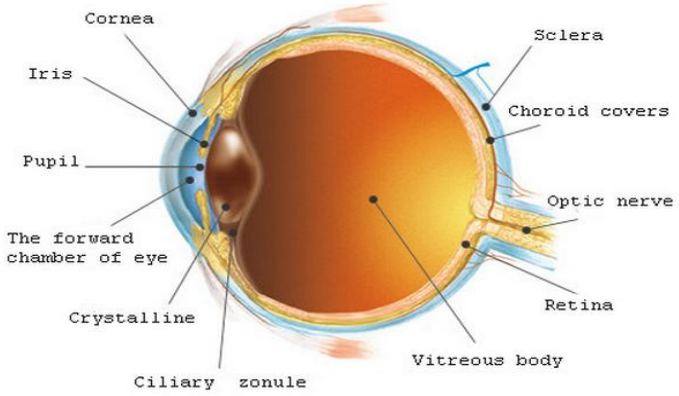


Figure 2 Human eye structures [2]

Light waves from an object enter the eye first through the cornea, which is the clear dome at the front of the eye. It is like a window that allows light to enter the eye. The light then progresses through the pupil, the circular opening in the center of the colored iris. Fluctuations in the intensity of incoming light change the size of the eyes pupil. As the light entering the eye becomes brighter, the pupil will constrict (get smaller), due to the pupillary light response. As the entering light becomes dimmer, the pupil will dilate (get larger).

Initially, the light waves are bent or converged first by the cornea, and then further by the crystalline lens (located immediately behind the iris and the pupil), to a nodal point (N) located immediately behind the back surface of the lens. At that point, the image becomes reversed (turned backwards) and inverted (turned upside-down).

The light continues through the vitreous humor, the clear gel that makes up about 80% of the eyes volume, and then, ideally, back to a clear focus on the retina, behind the vitreous. The small central area of the retina is the macula, which provides the best vision of any location in the retina. If the eye is considered to be a type of camera (albeit, an extremely complex one), the retina is equivalent to the film inside of the camera, registering the tiny photons of light interacting with it.

Within the layers of the retina, light impulses are changed into electrical signals. Then they are sent through the optic nerve, along the visual pathway, to the occipital cortex at the posterior of the brain. Here, the electrical signals are interpreted or seen by the brain as a visual image.

## 1.4 Corneal Geography

The corneal geography can be divided into four geographical zones from apex to limbus, which can be easily differentiated in colour corneal videokeratoscopy; the first is the central zone (4 central mms) which is almost spherical and called apex on which keratometry is based. Also it is called the optical or apical zone since the pupil allows only the rays passing through this area to reach the retina, then the paracentral zone: where the cornea begins to flatten, then the peripheral zone and the limbal zone.

The thickness of the cornea is bout 0.52mm in the axial area and about 0.66mm in the mid peripheral part so the cornea is flattering the periphery and becomes progressively flatter away from the center rendering the surface aplanatic.

The radius of curvature of anterior surface or axial zone of the cornea is 7.8mm and the radius of curvature of the posterior surface of the cornea is 6.7mm.

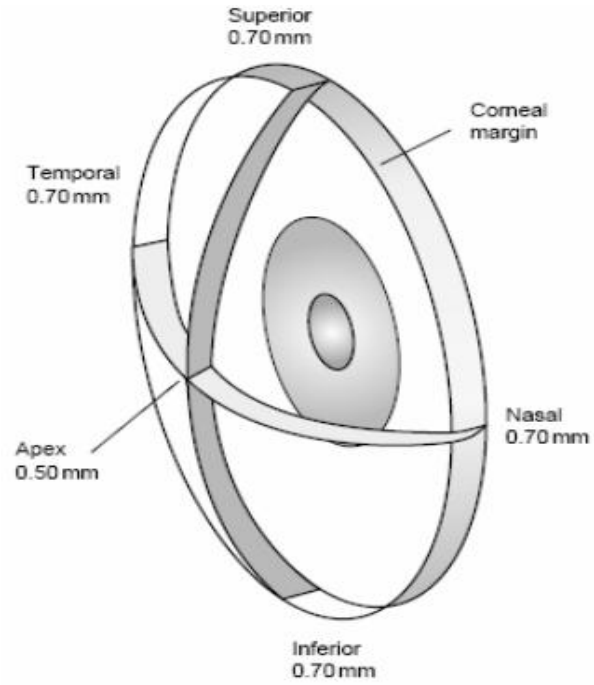


Figure 3 Corneal Geography[1]

## 1.5 Some disorders & diseases

### 1.5.1 Myopia, Hyperopia & Astigmatism

If the incoming light from a far away object focuses before it gets to the back of the eye, that eyes refractive error is called myopia (nearsightedness). If incoming light from something far away has not focused by the time it reaches the back of the eye, that eyes refractive error is hyperopia (farsightedness). In the case of astigmatism, one or more surfaces of the cornea or lens (the eye structures which focus incoming light) are not spherical (shaped like the side of a basketball) but, instead, are cylindrical or toric (shaped a bit like the side of a football). As a result, there is no distinct point of focus inside the eye but, rather, a smeared or spread-out focus. Astigmatism is the most common refractive error in cornea.

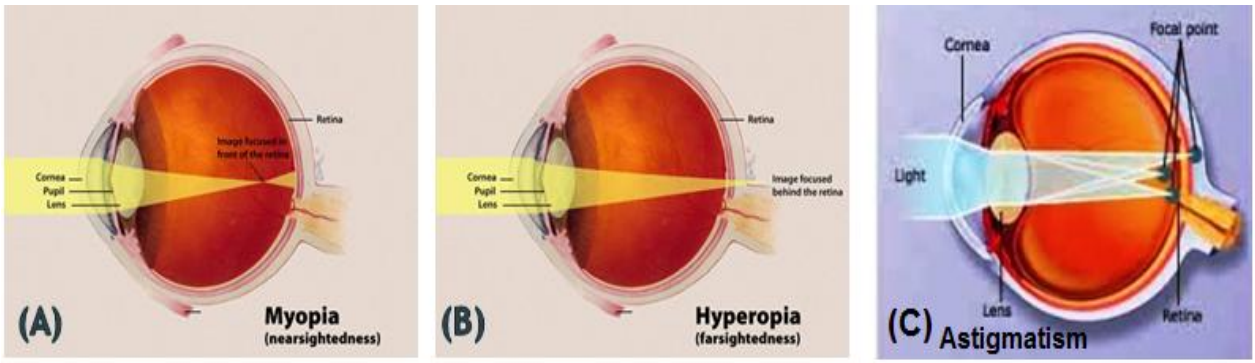


Figure 5 Some eye disorders: (a): Myopia, (b): Hyperopia, (c): Astigmatism.[2]

### 1.5.2 Keratoconus

Keratoconus is a progressive, non inflammatory disorder characterized by central thinning and steepening of the corneal curvature.

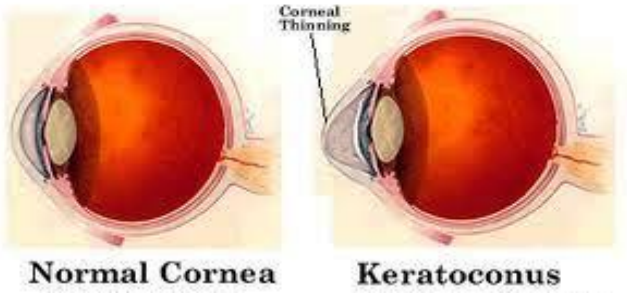


Figure 4 Keratoconus.[2]

This nature of keratoconus leads to increased myopia and irregular corneal astigmatism, which decrease visual acuity and visual quality. The reduced visual quality leads many patients with keratoconus to refractive surgery.

## 1.6 Some instruments to measure the corneal surface

The ideal cornea is of a circular base over which an utter dome is fitting. Its shape is flatter at the edges and steeper at the centre to improve quality of the inverted image, also the normal corneal surface is smooth and a healthy tear film (the layer of tear covering the outer anterior corneal surface) , can neutralize corneal irregularities. The corneal anterior surface acts as a transparent convex mirror reflects the incident light. Most of the corneal topographical instruments has been developed basing upon this fact; to measure the corneal surface by assessment of this corneal surface.

From Keratometry to keratoscopy till computerized videokeratoscopy (Modern Corneal topography) the measurement of the corneal surface witnessed a rapid developments and wide change during the last century. Chapter two discusses the principles and techniques on which the instrumentation of corneal topography is based. The only thing that is common among all these techniques is being a "Non-invasive technologies" for some uses a light target (lamp, LED, Plasido disc, etc.) and a microscope or other optic systems to measure corneal reflex of these light targets and mapping the corneal surface.

Modern corneal topographers use different methods for measuring the corneal surface like:

**Plasido system** (small cone or large disk) are the most popular.

Plasido cone with arc-step mapping (Keraton from Optikon2000).

Plasido disk with arc-step mapping (Ziess Humphery from Atlas).

**Slit- lamp topo-pachemetry** (Orbscan Buach and lomb).

**HR Pentacm** (Pentacam).

**Fourier Profilometery** (Euclid Systems cooperation ET-800).

**Laser interferometry** (Experimental method, it measures the interference pattern generated on the corneal surface by interference of two lasers or coherent wavefront).

Figure 5 A shows one of the latest corneal topographical instruments , while B shows a simple keratometer.

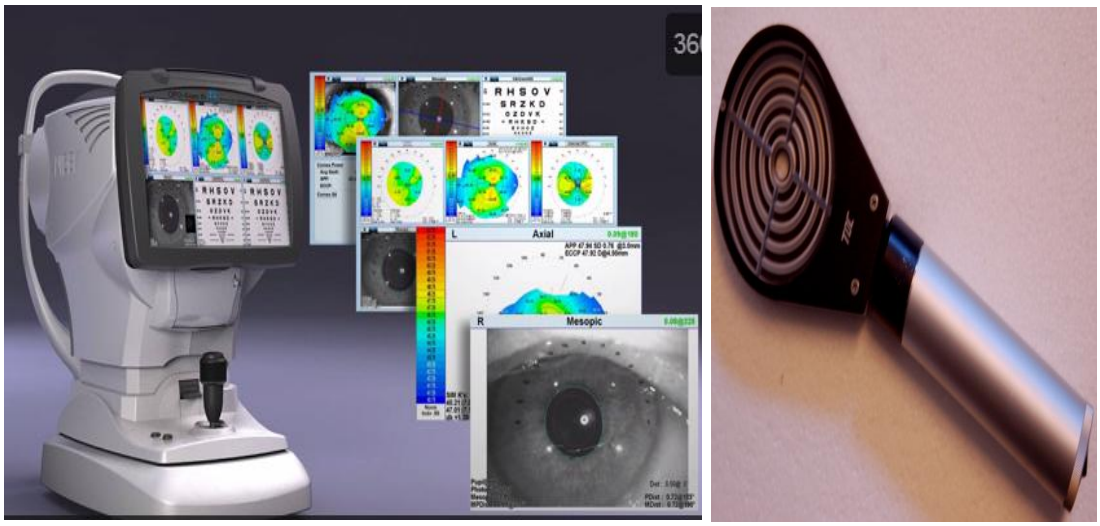


Figure 5 A: Modern photokeratoscopy scanner (OPD Scan III) & B: Placido disc keratoscope.[1]

## 1.7 Corneal topography

Corneal topography, also known as photokeratoscopy or videokeratography, is a non-invasive medical imaging technique for mapping the surface curvature of the cornea, the outer structure of the eye. Since the cornea is normally responsible for some 702699447\% of the eye's refractive power, its topography is of critical importance in determining the quality of vision and corneal health.

The three-dimensional map is therefore a valuable aid to the examining ophthalmologist or optometrist and can assist in the diagnosis and treatment of a number of conditions; in planning cataract surgery and intraocular lens (IOL) implantation (plano or toric IOLs); in planning refractive surgery such as LASIK, and evaluating its results; or in assessing the fit of contact lenses.

Corneal topography instruments used in clinical practice most often are based on Placido reflective image analysis. This method of imaging of the anterior corneal surface uses the analysis of reflected images of multiple concentric rings projected on the cornea.

Within the past 10 years, corneal topography has grown from an elaborate and costly device used only for clinical research in large institutions to a critical in-office tool that many optometrists now use daily. Along with advances in computerization and software development, topographers have become smaller, more compact, more affordable and more precise. This primer describes the mechanics, methods of interpreting the data, and indications for performing corneal topography.

A development of keratoscopy, corneal topography extends the measurement range from the four points a few millimeters apart that is offered by keratometry to a grid of thousands of points covering the entire cornea. The procedure is carried out in seconds and is completely painless.

## 1.8 Principles of Corneal topography

Multiple light concentric rings are projected on the cornea. The reflected image is captured on a charge-coupled device (CCD) camera. Computer software analyzes the data and displays the results in various formats. Most corneal topographers evaluate 8,000 to 10,000 specific points across the entire corneal surface. By contrast, keratometers measure only four data points within the cornea's central 3-4mm; the small size of this area can lead to errors in determining precise toricity. Topography provides both a qualitative and quantitative evaluation of corneal curvature.

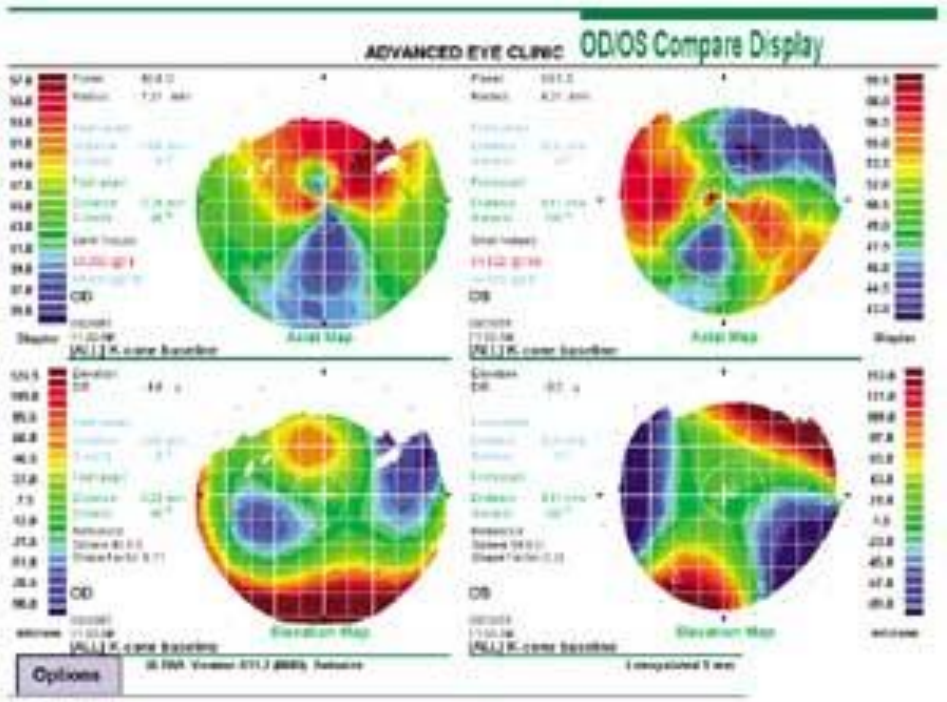


Figure 6 Elevation and axial maps with some indices.

It does so by utilizing concentric rings, which project onto the cornea to create a virtual image. The device compares this image to the target size, and the computer then calculates the corneal curvature.

Although many different systems are available, all share some unifying measurement characteristics. The computerized topographer can generate various graphical representations.

When performing corneal mapping for diagnosis of conditions and/or contact lens fitting, the two most common maps that practitioners use are:

## 1.9 Topographic Maps

### 1.9.1 Axial Map

Also called the "power" or "sagittal" map, this output is the simplest of all the topographical displays. It shows variations in corneal curvature as projections and uses colors to represent dioptric values. Warm colors such as red and orange show steeper areas; cool colors such as blue and gree denote the flatter areas. The axial map gives a global view of the corneal curvature as a whole. Its downside is its tendency to ignore minor variations in curvature.

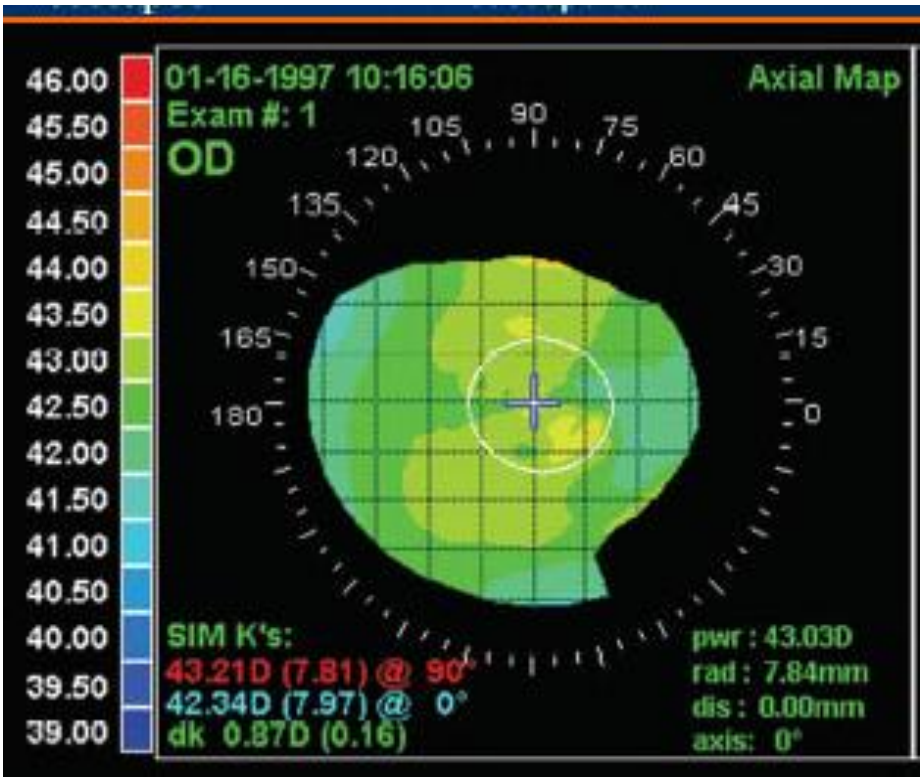


Figure 7 Axial map

### 1.9.2 Tangential map

Sometimes referred to as the instantaneous, local, or "true" map, it also displays the cornea as a topographical illustration, using colors to represent changes in dioptric value. However, the tangential strategy bases its calculations on a different mathematical approach that can more accurately determine the peripheral corneal configuration. It does not assume the eye is spherical, and does not have as many presumptions as the axial map regarding corneal shape. In fact it is the map that more closely represents the actual curvature of the cornea over the axial map.

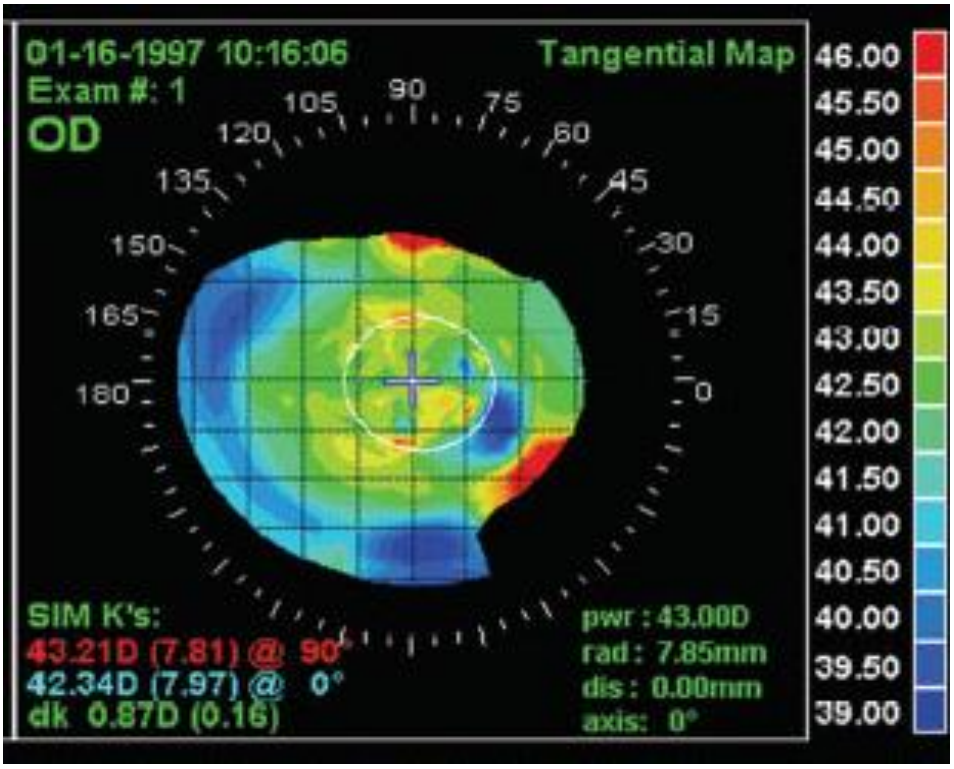


Figure 8 Tangential map.

The tangential map recognizes sharp power transitions more easily than the axial map, and eliminates the "smoothing" appearance that appears on the axial map. This is not universally true for all topographers. Compared with axial maps, tangential maps yield smaller patterns with details that are more centrally located. Tangential maps also offer a better visualization

of the precise location of corneal defects. This display is most useful in following trends in the postsurgical or pathologic eye.

### 1.9.3 Elevation map.

This utilizes yet another algorithm to give additional information about the cornea. An elevation map shows the measured height from which the corneal curvature varies (above or below) from a computer-generated reference surface. Warm colors depict points that are higher than the reference surface; cool colors designate lower points.

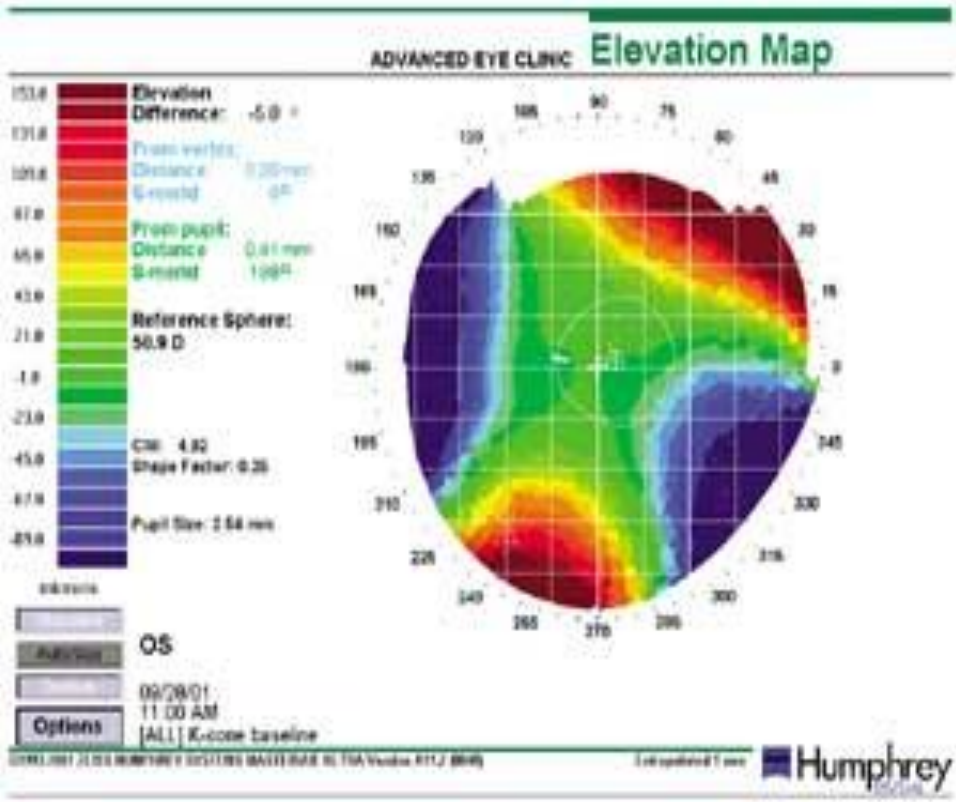


Figure 9 Elevation map.

This map is most useful in predicting fluorescein patterns with rigid lenses. Higher elevations (reds) represent potential areas of lens bearing, while the lower areas (greens) will likely show fluorescein pooling.

### 1.9.4 Refractive map

This utilizes the measured dioptric power and applies Snell's law to describe the cornea's actual refractive power.

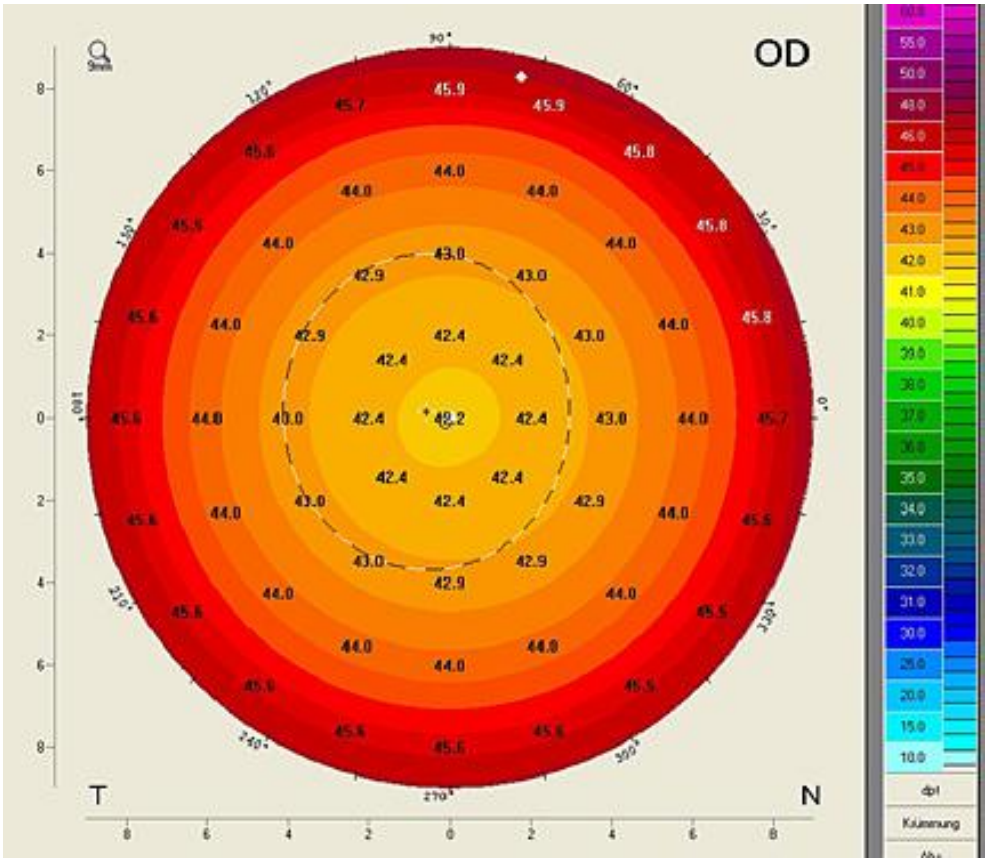


Figure 10 Spherical refractive map

A refractive map compensates for spherical aberrations as well as the aspheric contour of the cornea. The central portion of the refractive map is most important. This area overlies the pupil, so aberrations here almost invariably impact visual performance.

Clinicians use refractive maps to evaluate visual performance in post-refractive surgery patients. This view identifies central islands in patients who have undergone PRK or LASIK.

## 1.10 Topographic Scales

Two basic scales are commonly used (absolute and relative scales). The absolute or standard scale which assigns a specific color to each dioptric value and constrains the data to fit within that range. Clinically use standard maps when comparing two different eyes or comparing the same eye over time . Because the steps are in large increments (generally 0.5 D), their disadvantage is that they do not show subtle changes of curvature and can miss subtle form of keratoconus.

The relative scale (auto-size, or normalized scales) which subdivides the cornea into dioptric intervals based on its actual curvature range (usually a 6.00D range).

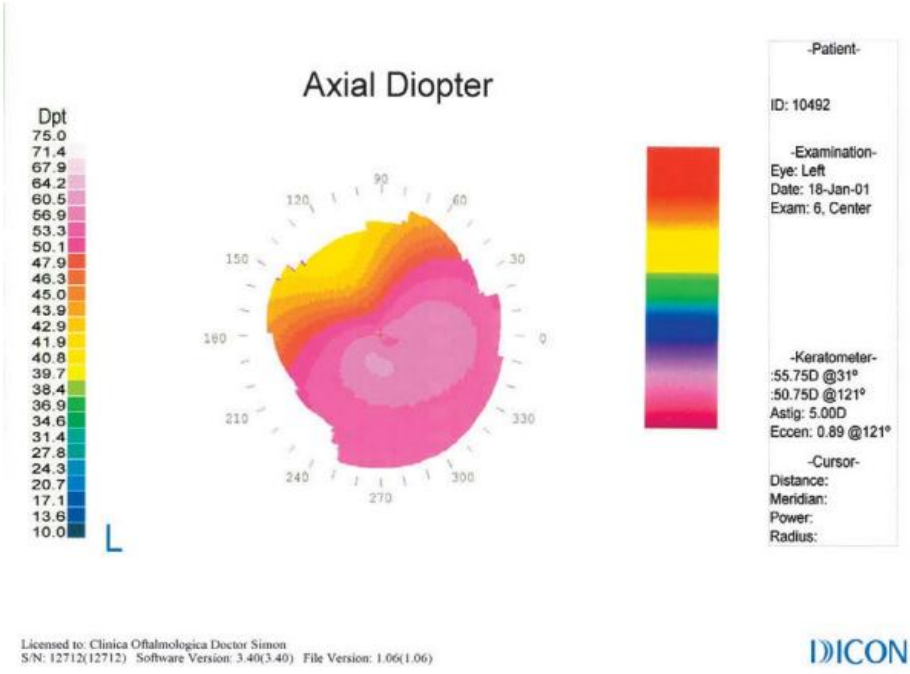


Figure 11 Absolute scale in KC.

The actual colors are not specific to a dioptric value when using the normalized scale, but are relative to that particular patient's eye. Clinically use normalized (relative)maps when evaluating one particular eye, the disadvantage is that the colours of 2 different maps cannot be compared directly and have to be interpreted based on the keratometric values of their different colours scales.

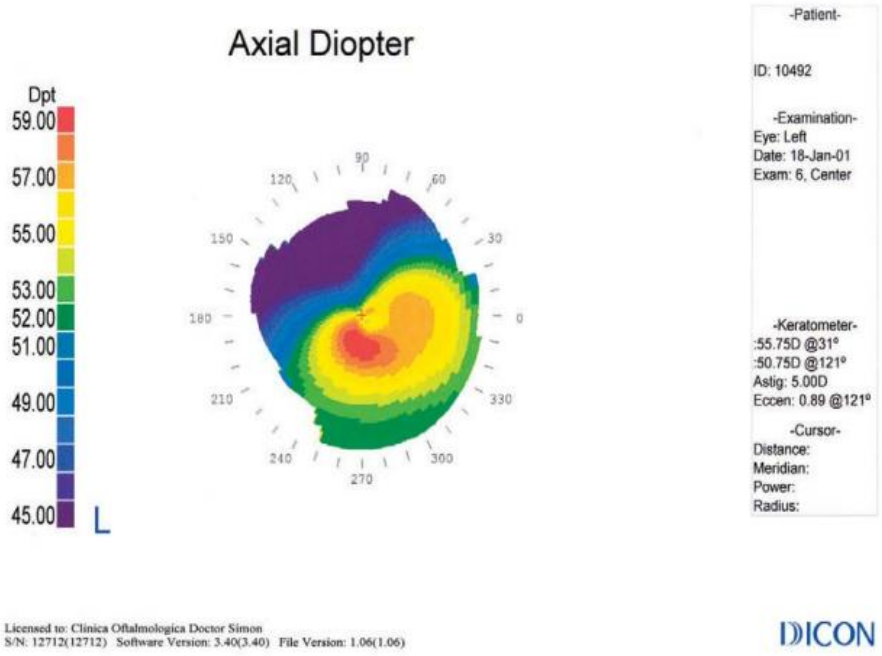


Figure 12 Normalize scale in KC.

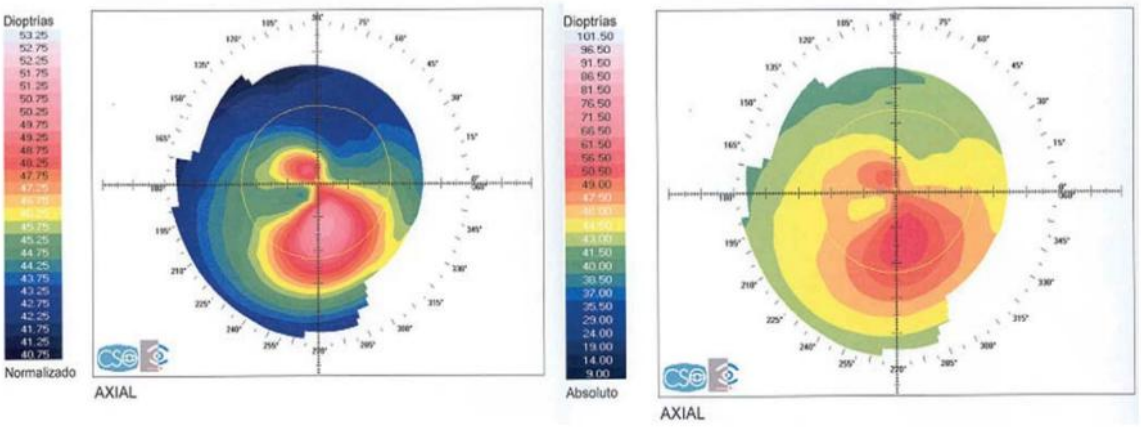


Figure 13 Corneal topography of an eye with keratoconus using A) normalized(0.25 D) & B) absolute (1.5 D) scales.

.

Quantitative descriptors of corneal topography consist of indices generated from artificial intelligence programs that facilitate interpretation of topographic information. Different manufacturers offer alternative programs designed to increase the utility of these instruments for clinical and research analyses.

## 1.10 Comparison of corneal topographic mapping

### 1.10.1 Absolute maps

This scaling system has a preset color scale with the same dioptric steps, dioptric minimum and maximum assigned to the same colors for a particular instrument. These maps allow direct comparison of 2 different maps. However, because the steps are in large increments (generally 0.5 D), their disadvantage is that they do not show subtle changes of curvature and can miss subtle local changes (e.g., early keratoconus).

### 1.10.2 Normalized maps

This scaling system has different color scales assigned to each map based on the instrument software that identifies the actual minimal and maximal keratometric dioptric value of a particular cornea. The dioptric range assigned to each color generally is smaller compared to the absolute map; consequently, maps show more detailed description of the surface. The disadvantage is that the colors of 2 different maps cannot be compared directly and have to be tg6interpreted based on the keratometric values from their different color scales.

## 1.11 Mean shape of the human cornea

**A)**Viewed from the front, the cornea is slightly oval with:

1- vertical and horizontal dimensions of approximately 11 and 12 mm, respectively.

2- Normally, pupil diameter ranges from 3-6 mm,and this limits the optical zone of the cornea to the central 6 mm under most conditions.

**B)** In profile:

1- most corneas are nearly circular near the center, with an average apical radius ofcurvature of about 7.8 mm.

2- The normal range is 7-8.5 mm.

3- The horizontal radius is usually 0.05-0.25mm flatter than the vertical, This equates to 0.25-1.25 diopters (D) of corneal astigmatism; average corneal astigmatism is about 0.70 D. In general, the mean apical radius decreases with higher myopia.

The anterior cornea is the major refractive surface of the eye, and is responsible for over two thirds of its total dioptric power. Therefore, very small changes in corneal shape resulting from surgery or disease can have a dramatic effect on the clarity with which an image is brought to a focus on the retina.

# CHAPTER 2
# LITRATURE REVIEW

**Amar Agarwal** explained corneal topography and its fundamentals in [1]. They discussed topics like post-LASIK ectasia and decentred ablation and covered various topographic machines like ORBSCAN and the PENTACAM. The PENTACAM chapter is of significant importance to my work because my data base is PENTACAM topographic images. This book also covered other related topics; such as anterior segment OCT and the aberometers as they are complementary to the topographic machines.

**T.Reinhard** edited [2] as the "Cornea and External Disease" volume, which covers the recent developments related to the cornea, with a discussion of diagnostic measures and treatment emphasis. The series of "Essentials in Ophthalmology" is a new review series covering all of ophthalmology categorized in eight subspecialties. All the covered topics by the book are of direct clinical relevance aims to contribute to the development of optimal diagnostic and therapeutic procedures for patients with disease of the cornea.

**Kara Rogers** introduced a new way to see the human eye in [3]. The newly discovered methods in diagnosing and treating eye diseases and disorders. The ninth chapter contains detailed information about diagnosis and treatment of eye diseases, and further details about optical aids and corrective surgeries.

A modern understanding of the underlying physiology of primary astigmatism and the pathology of astigmatism associated with disease and trauma was presented in [4] by **Michael Goggin**. It explores many therapeutic approaches to amelioration of the effects of astigmatism in its many forms by surgical and optical means. This book covers etiology, types, classification and diagnosis of astigmatism.

**Melanie C.Corbett** in [5] presented corneal topography in different way; browsing its basic principles and applications to refractive surgery and classifying its various types according to the working and measurement principle. An investigation of complications of post-refractive surgery cases was presented and discussed with the aid of topographic patterns examples.

**Jack T. Holladay** introduced a method of keratoconus detection using corneal topography in [6] by reviewing the topographic patterns associated with keratoconus suspect patients and providing criteria for keratoconus screening. The method used by them is a case study using maps from the NIDEK OPD-Scan II and OPD Station to highlight patterns seen in keratoconic corneas.

**Ke Yao** provided in [7] a comparison among astigmatism, high order aberrations, and optical quality of the cornea after micro-incision (~1.7 mm) versus small incision (~3.2 mm) in their research aiming to evaluate the topical quality of the cornea by a clinical study included micro-incision cataract surgery and small incision cataract surgery performed on 60 eyes. Corneal astigmatism and higher order aberrations to the sixth order were measured also using the NIDEK OPD-Scan topographer.

**Keith J.Croes** illustrates the breakthrough method in astigmatism analysis in [8], called "Alpins Method". A well known method designed and developed by Noel Alpins to assist in planning and evaluation of corneal refractive surgery for people with astigmatism.

**Michael W.Belin** presented a study on detecting keratoconus and performing topographic screenings prior to refractive surgery in [9] as a discussion of corneal topography and Scheimpflug imaging. This study is important because the means by which to determine the cornea's true shape is still evolving and has proven more problematic and for the need to understand topography in order to screen patients properly and may at times have to choose a procedure (LASIK, sur-face ablation, conductive keratoplasty, phakic IOL) or elect not to proceed based on topographic findings.

**Michael W.Belin** presented [10] as the Belin / Ambrósio Enhanced Ectasia Displayis has been added to the software of the PENTACAM. The first comprehensive refractive surgical screening tool to be fully elevation based. The goal of the software is to assist the refractive surgeon in identifying those patients who may be at risk for post-operative ectasia and/or to assist in the identification of early or subclinical keratoconus; by utilizing information from both the anterior and posterior corneal surfaces.

**Damien Gatinel** described the effect of the corneal asphericity and toricity on the map patterns and best fit sphere (BFS) characteristics in elevation topography in [11]. The corneal

surface was modeled in this study as a biconic surface of principal radii and asphericity values. The apex of the biconic surface corresponded to the origin of a polar coordinates system. The squared residuals was minimized to calculate the values of the radii of the BFSs and apex distance (A-values:z distance between the corneal apex and the BFS) of the modeled corneal surface for various configurations relating to commonly clinically measured values of apical radius, asphericity and toricity.

**Rajeev Jain** introduced [12] to explain the Scheimpflug imaging principle as a basic imaging acquisition in PENTACAM. Also they mentioned the instrumentation of Scheimpflug imaging and the method of image acquisition by PENTACAM, and screening procedures of diseases like keratoconus and glaucoma.

**Michael W. Belin**; introduced [13] as a monograph based on an informational symposium. The symposium included the explanation of diagnostic capabilities of the PENTACAM as a comprehensive eye scanner as well as how best to integrate this pioneering instrument into clinical practice.

**Ye Han** suggested a mathematical model to correct myopic astigmatism in [14]. The corneal surface was modelled as a torus before ablation and as a sphere after ablation in the myopic astigmatism eye. In other words the mathematic model to determine the ablation profile in refractive surgery was deduced according the two surfaces. The two different-radii of curvature of the torus along its perpendicular meridians were determined by the deepest and flattest section of the corneal measure by topographic observation. This mathematic model was applied in the software of the ophthalmic EXCIMER laser system to correct refractive error.

**Liliane Ventura** had developed an automatic optical system attached to the Slit Lamp in [15]; providing an automatic measurements of the radius of curvature of the cornea at low cost. The system is able to measure irregular astigmatism and the clinician is able to understand the behaviour of the cornea's curvature radius in these regions by the comparison of the graphical analysis of regular astigmatism that is generated by the software. It was introduced when there was no system commercially available which is able to measure irregular astigmatism. The system's precision is 0,005mm for the curvature radius and 2' for the axis component.

**Michael D. Twa** introduced an automated decision tree classification of corneal shape in [16]. This work describes the application of decision tree induction, an automated machine learning classification method, to discriminate between normal and keratoconic corneal shapes in an objective and quantitative way. Corneal surface in this work was modelled with a $7^{th}$ order Zernike polynomial for normal eyes as well as eyes diagnosed with keratoconus. A C4.5 algorithm is used as decision tree classifier. Also this method was compared with other known classification methods.

**Fatemeh Toutounchian** proposed a method for detection of keratoconus and suspect keratoconus by machine vision in [17]. They focus on developing artificial intelligence tool to diagnose Keratoconus. This artificial intelligence algorithm finds Keratoconus by employing features of topographical map of eye. These features are obtained by Pentacam and extracted by topographical images of eye via image processing techniques. Their final result shows that they could detect Keratoconus, suspect to Keratoconus and normal eye by the proposed algorithm.

A spatial modeling and classification of corneal shape was suggested by **Keith Marsolo** in [18]. This classification provide a comprehensive follow-up to the work in [16], examining a second representation, pseudo-Zernike polynomials, for determining the change in classification accuracy. A comparison of the fidelity of both methods was illustrated using residual root-mean-square (rms) error and an evaluation of accuracy using several classifiers: neural networks, C4.5 decision trees, Voting Feature Intervals, and Na¨ıve Bayes. We also examine the effect of several meta-learning strategies: boosting, bagging, and Random Forests (RFs). They show that classification accuracy is similar for multi-class datasets and data transformations, but differs by classifier. This work concluded that the Zernike polynomials provide better feature representation than the pseudo-Zernikes and that the decision trees yield the best balance of classification accuracy and interpretability.

Refractive error detection via group sparse representation was proposed in [19] by **Qin Li** this approach presents an effective computer aided diagnosis of astigmatism. It also presented a system consists of two major steps: the first is image segmentation and geometrical feature extraction achieving high accuracy of segmentation for images at poor quality caused by distortion during image digitization.; and the second is group sparse representation based

classification to avoid misclassifications by incomplete information.. The experimental results demonstrate the feasibility of the new classification scheme with good performance for potential medical applications.

Estimation of Corneal topography that is based on the Placido disk principle depends on good quality of precorneal tear film and a wide eyelid aperture to avoid reflections from eyelashes. [20] Is a study and approach for enhancing the standard operating range of a placido disk videokeratoscope for corneal surface estimation suggested by **Weaam Alkhaldi** This enhancment was achieved by corporating in the instrument' topography estimation algorithm with an image processing technique that comprises a polar-domain adaptive filter and a morphological closing operator.

A computationally efficient interference detection method in videokeratoscopy images was introduced by **David Alonso-Caneiro** in [21]. This paper presents a set of algorithms for detecting interference patterns in videokeratoscopic images is presented. First a frequency approach is used to subtract the background information from the oriented structure followed by gradient-based analysis to obtain the pattern's orientation and coherence. Detecting videokeratoscopic pattern interference is important when assessing tear film surface quality, break-up time and location as well as designing tools that provide a more accurate static measurement of corneal topography.

[3] References were stated above discussing the anatomy, structure and pathology of the cornea as an impact tissue in the human eye; affects the process of vision .and defines its quality.

[5] References were selected and stated above providing understanding to the healthy and abnormal structure of the human eye.

A total number of [10] references reviewed and stated above. Also a background of how these corneal topographic images are calculated and what are the methods used to determine the correction of abnormal corneas; They also include more information PENTACAM (the instrument from which the data base was collected) are essential to the proposed work.

The remaining literature is of two parts:

**A)** Researches that tried to analyze, diagnose or simulate the topographic images from mathematical, technical and engineering view. And researches which investigated in the accuracy and reliability of the topographic imaging techniques; those are (10) references.

**B)** Researches and books that illustrate other methods diagnose astigmatism and keratoconus or try to differentiate between them; and those are a collection of (7) references.

This review involves 21 references and covered 4 sections of the main topic as explained by the summary, each reference can serve more than one purpose; overlapping is there.

From this review it's clear that no previous researches have been done in this area using the digital image processing techniques. The algorithm proposed in this thesis is novel.

# CHAPTER 3
# PENTACAM

## 3.1 Pentacam

PETACAM ocular scanner is a combined device consisting of a slit illumination system and a Scheimpflug camera which rotates around the eye. This instrument is considered as specialized camera for different ophthalmic applications. It utilizes Schiempflug principle as a non-invasive medical imaging technique for mapping the surface curvature of the cornea, and performing full analysis of the anterior segment.

Figure 14 The Pentacam instrument from Oculus®

### 3.1.1 Working principle:

Pentacam is a “Reflection- based corneal topographic system”. Reflection-based systems work by taking cut sections in the cornea; both of its anterior & posterior surfaces & thickness in-between the m are measured. A thin layer within the eye is illuminated through the slit. Corneal cells are not entirely transparent; so they scatter the slit light. And create a sectional image which is then photographed in side view by a camera. This camera is oriented according to the Scheimpflug principle, hence creating completely shar image of the

illuminated plane that appears from the anterior surface of the cornea right up to the posterior surface of the crystalline lens.

This camera rotates around the camera 360° in 2seconds to capture 50 images for the surface of cornea, all are cantered at the cornea centre. Meanwhile, the slit-camera device generates a series of radially oriented images of the anterior eye chamber. In the subsequent analysis of the sectional images, tissue boundaries are detected and point clouds are assigned to the various tissue layers (anterior and posterior corneal surfaces, iris, crystalline lens).

The sectional images are saved, corrected in relation to a common reference point and then put together to create a three-dimensional model of the entire anterior eye chamber. This makes it possible to generate reproducible tomographic images of the anterior eye chamber in any desired plane.

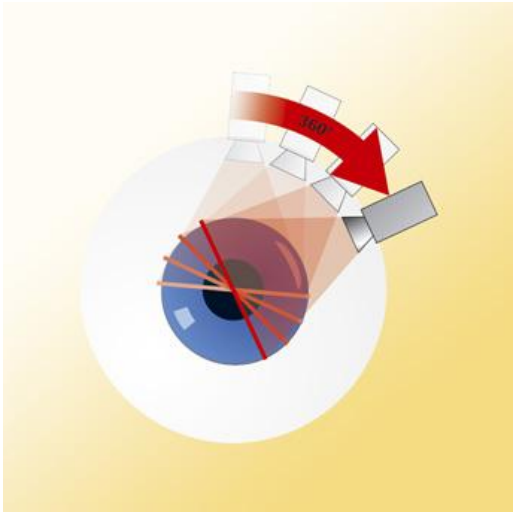


Figure 15 Rotating Schiempflug camera in the Pentacam

After correction for Scheimpflug distortion and light refraction at tissue interfaces the exact of location of image edge points in the eye is determined by means of ray-tracing. Eye movements during image acquisition are captured by a second camera (pupil camera) and also taken into account in the mathematical evaluation.

This produces a set of 3D- measurement data which gives a precise geometric description of the anterior eye segment. This data in turn can be used to generate data on elevation,

curvature, pachemetry, depth of the anterior eye chamber…etc. in the well-known form of colour maps.

The Pentacam® is the only instrument which is able to perform a precise and complete measurement and analysis of the entire cornea and its centre. The rotating measurement principle avoids measurement errors that may result from horizontal scanning. The density of data points is greatest at the centre due to the radial orientation of the sectional images.

### 3.1.2 Technical data

The instrument from which the data base of this work has been collected has the following specifications; as provided by the manufacturer:

Table 1Technical data by Pentacam Model; A) Features & B) Measurements

**A) Features**

| | |
|---|---|
| Camera | digital CCD camera |
| light source | blue LEDs (475 nm UV-free) |
| Processor | DSP with 400 mil. operations/s |
| Speed | 50 images in 2 seconds delivering 500 true elevation values each 1) |
| dimensions (W x D x H) | 280 x 360 x 505-535 mm<br>(11 x 14 x 20-21 in) |
| Weight | 10,5 kg (23.1 lbs) |

**B) Measurements**

| | |
|---|---|
| Curvature | 3 - 38 mm<br>9 - 99 dpt |
| Precision | ± 0,2 dpt |
| Reproducibility | ± 0,2 dpt |
| Operating distance | 80 mm |
| Max. Power consumption | 50 W |

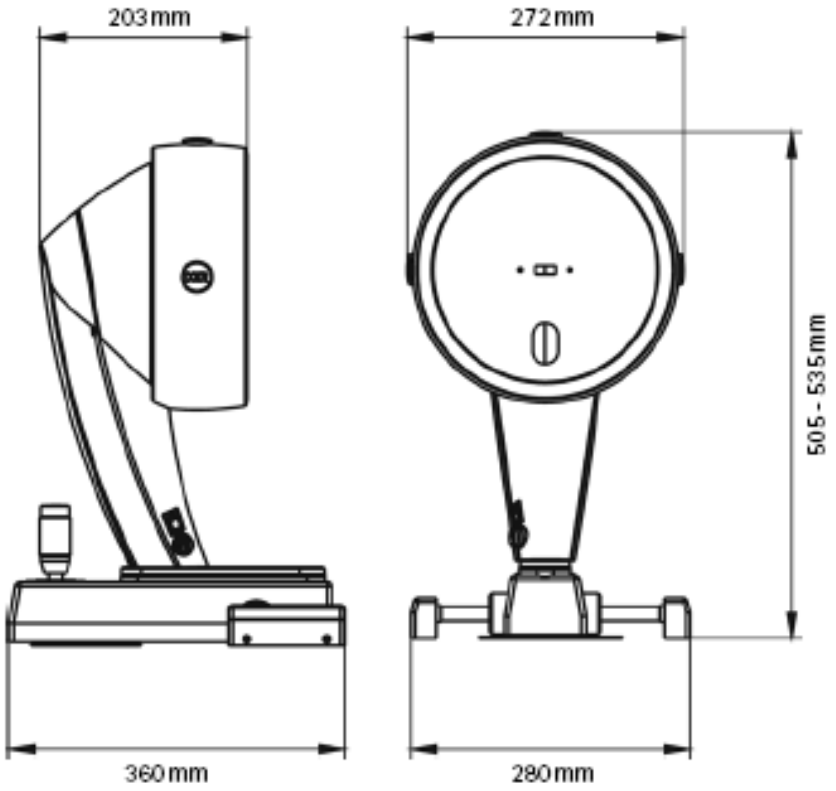


Figure 16 Technical drawing of Pentacam

As the details shows, this instrument has a high quality images. With one scan it can provid:

• Scheimpflug pictures out of 25,000; all are true elevation points
• 3D anterior segment analysis for implanting phakic lenses and glaucoma check-up
• Pachymetry from limbus to limbus –over the entire cornea
• Topography of anterior and posterior surface of the cornea
• Cataract analysis by objective densitometry quantification
• Tomography of the anterior eye segment as a virtual 3D model

What are important and related to this work are the higher topographical capabilities, the high precision and quality of Pentacam images (colour coded maps) and the unharmed technology as well as the ease of use and availability. Those are the reasons behind selecting the Pentacam as the source instrument. Physicians interpret the colour coded images to diagnose & treat patients with eye refracting issues manually; this work is a try to make this process computerized by means of image processing techniques.

### 3.1.3 Pentacam sample image

Figure below shows one of the images was provided by Randhawa Eye Hospital (Patiala/ Punjab) as input data to apply the proposed algorithm.

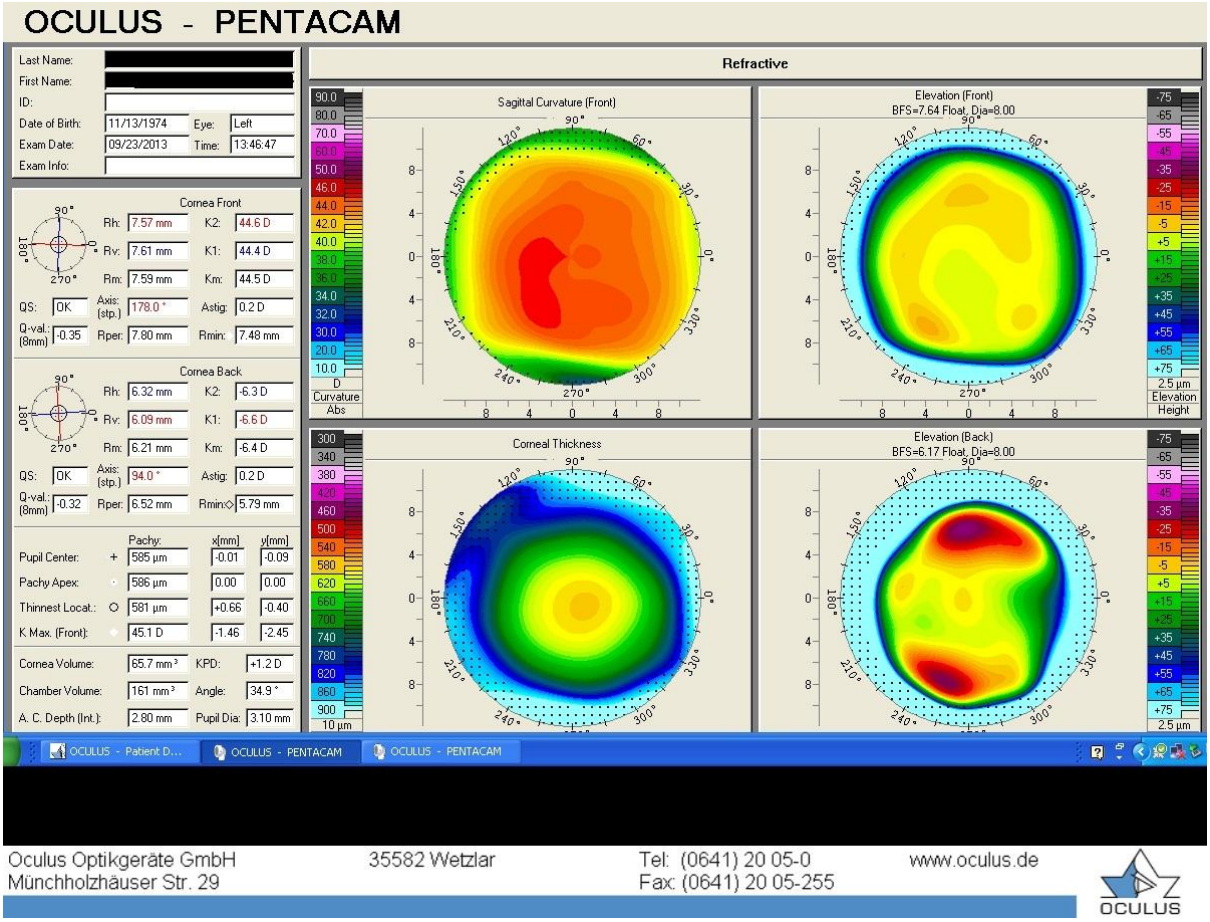


Figure 17 Sample image from Data base.

This image shows a refractive view of the corneal topography, the scale used while taking the image (performing the corneal test on the patient's eye) is absolute, which allows the comparison among other images scanned using the same scale and hence the classification and the proposed algorithm can be applied.

The upper left map is the axial curvature map on which this algorithm is applied. The right upper and lower maps are the front and back corneal surface elevation maps ( doctor use them to assure the correct diagnosis). The down left map is pachemetry data or the corneal thickness map shows the overall thickness in μms. Each map has its own colour scale and step.

## 3.2 Astigmatism diagnosis

Astigmatism is caused by a disorder in the eye in which the shape of the cornea is more oval and asymmetric than the normal round shape. This deformity causes the light to focus on in front of and/or behind the retina instead of the retina itself; causing images to be blurred or distorted. People with astigmatism also report headache and/or eye strain.

Blurred or distorted vision caused by astigmatism can be improved either by wearing glasses or contact lenses. The 100% curing solution to astigmatism is the painless refraction surgery (LAISK) or any other type of refractive surgery in which the surgeon has to be provided with precise information regarding the geometry of the eye (corneal & lenses shapes ).

### 3.2.1 Etiology

Total astigmatism can be divided into corneal (or keratometric) astigmatism, lenticular astigmatism, and retinal astigmatism. Most astigmatism is corneal in origin. Lenticular astigmatism is a result of uneven curvature and differing refractive indices within the crystalline lens. It is well accepted that there is some relationship between the eye's corneal and internal astigmatism. Prediction of the total astigmatism of the eye based on the corneal astigmatism.

### 3.2.2 Types and characterising astigmatism

A normal non astigmatic eye has a dome round shaped cornea with a uniform curvature, and hence; single refracting power all over its surface. In spherical errors (myopia and hyperopia) the cornea represent a small section of a bigger sphere or say "basketball" resulting in a uniform refractive power in all directions and equal power in all meridians (planes), while the astigmatic cornea tends to have a curvature in one meridian greater than another which makes the cornea represent a section of an oval shape or say "football" or "rugby ball" (each meridian is 90 degrees apart from the other) .

This specific geometry of the corneal surfaces causes light rays refracted by astigmatic cornea to be brought to more than a single point focus which makes the retinal image to be formed from a distant or/and near points rather than single sharp point.

Astigmatism is a very common eye disorder and it can occur either with near sight (myopia) or far sight (hyperopia); i.e. one eye can has two refractive errors in the perpendicular meridians; each one is a resultant of spherical error + astigmatic error. For example, the eye diagram shown in figure.2 is for a cornea having +2.5diopters in the 90 degrees meridian, and +1diopter in the 180 degrees meridian.

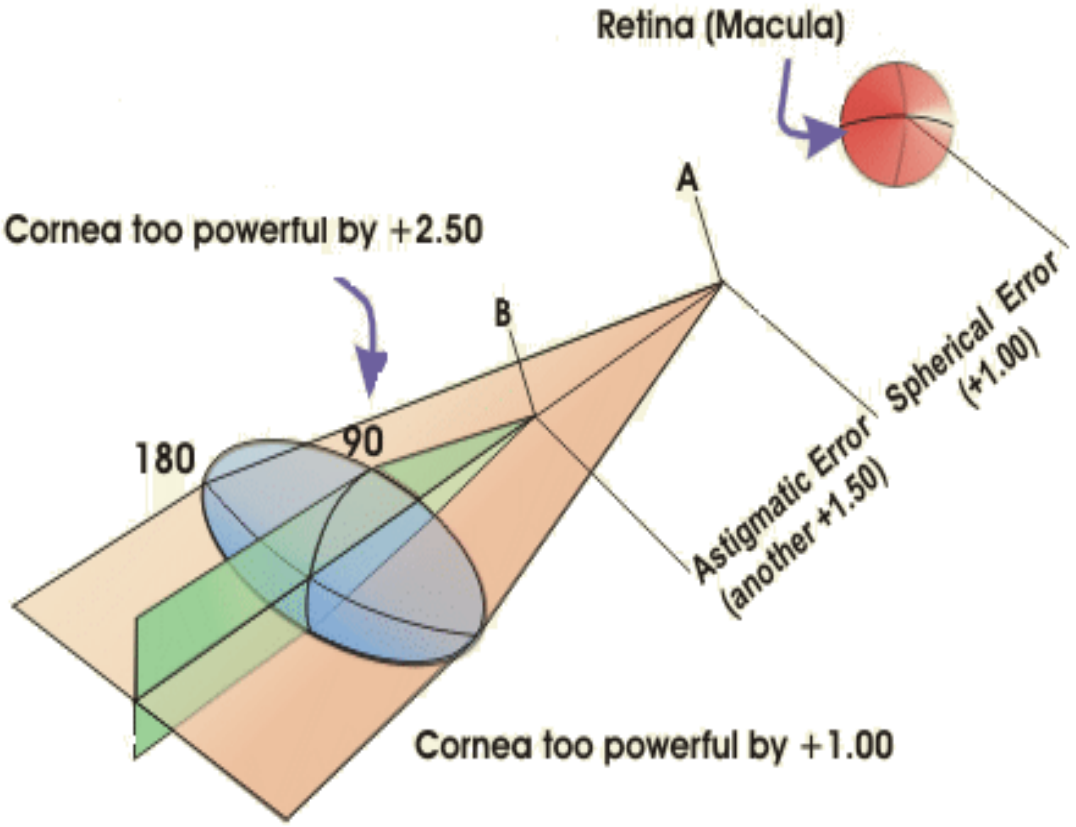


Figure 18 An example of spherical +astigmatic refractive error (this cornea is too powerful by+2.5D in the vertical meridian & too powerful by+1 in the horizontal meridian).

Corneal astigmatism is subdivided into regular astigmatism and irregular astigmatism.

Regular astigmatism is of five types:

1) Simple hyperopic astigmatism: the two perpendicular meridians focuses light in two different points, one behind the retina, and one on the retina.
2) Compound myopic astigmatism: both of the meridians bring light in foci in front of the retina.
3) Compound hyperopic astigmatism: both of the meridians bring light in foci behind the retina.
4) Mixed astigmatism: one meridian focuses light in front of the retina and the other behind it.

Regardless of the orientation of that bowtie shape; the two meridians maintain a seperation angle of 90 degrees between each other in regular astigmatism. And the position of meridians decides the type of regular astigmatism case. If the flat meridian is at or near the 180 degrees; the astigmatism is called “with the rule” as the case in Figure.4, and if it is at or near to 90 degrees; then it is called “against the rule astigmatism”.

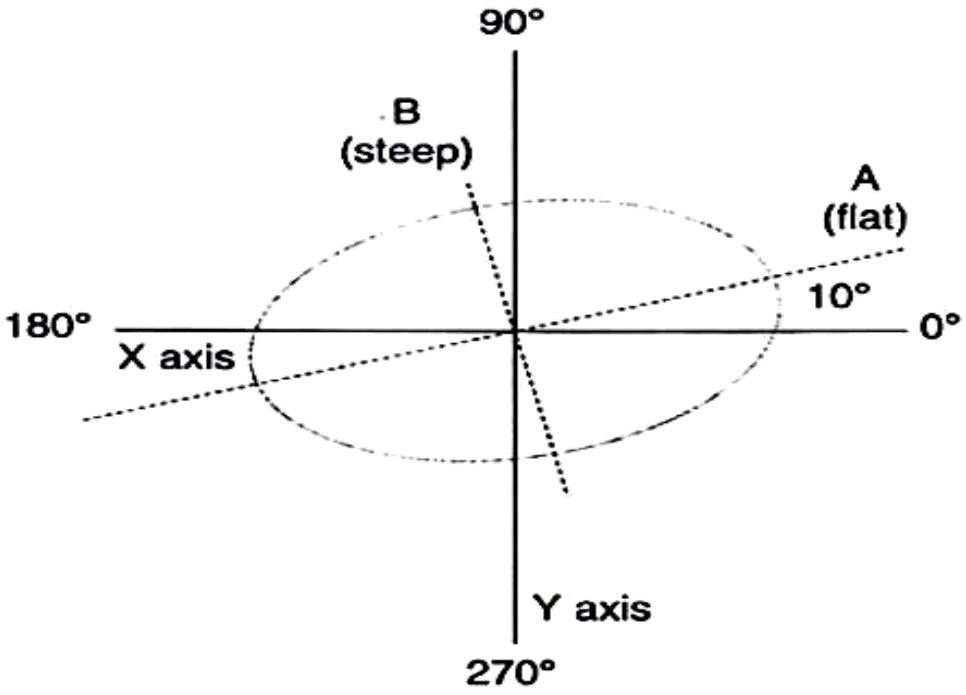


Figure 19 The elliptic base of the astigmatic cornea; A: is the flat meridian at 10degrees, & B: is the steep meridian at 190 degrees

On the other hand, irregular astigmatism is the case when two or more meridians are sperated by an angle which is not 90 degrees. Two or more steep hemimeridians are not located exactly oppostie to each other, the same case applies for falt hemimeridians

As topographic patterns: the corneas spherical refractive disorders still look round in shape, while corneas with astigmatic refractive errors look more oval or elliptic. This means that the slop of the astigmatic corneal dome is steeper at the short meridian, while the slop along with the long meridian is flatter. Figure 4 shows the base of astigmatic cornea along with the positions of long and short meridians in a regular astigmatism case.

All the types of regular astigmatism appear in the topographic patterns creating a “bowtie”or a “figure eight” with perpendicular meridians. One meridian is called the steep meridian which is the one of higher degree of curvature (smaller raduis of curvature & bigger diopter value) and the flat meridian is the one with less degree of curvature (bigger raduis of curvature & lesser diopter value).

### 3.2.3 Ideal Astigmatic topographic patterns

In this patient, the color changes turning inward right over the top of the pupil creating a “bowtie”, “figure eight” or “dumbbell appearance”. Vertical bowtie orientation is with-the-rule astigmatism or plus cylinder at ninety.

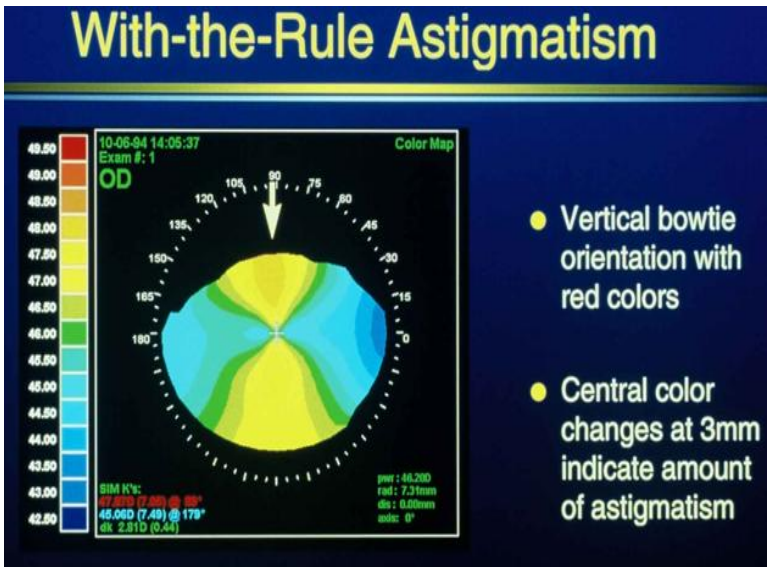


Figure 20 With the rule astigmatic pattern

When the bowtie assumes a horizontal orientation, it is known as against-the-rule astigmatism or plus cylinder at 180. The same approximations can be made here as in the with-the-rule astigmatism just in the opposite direction.

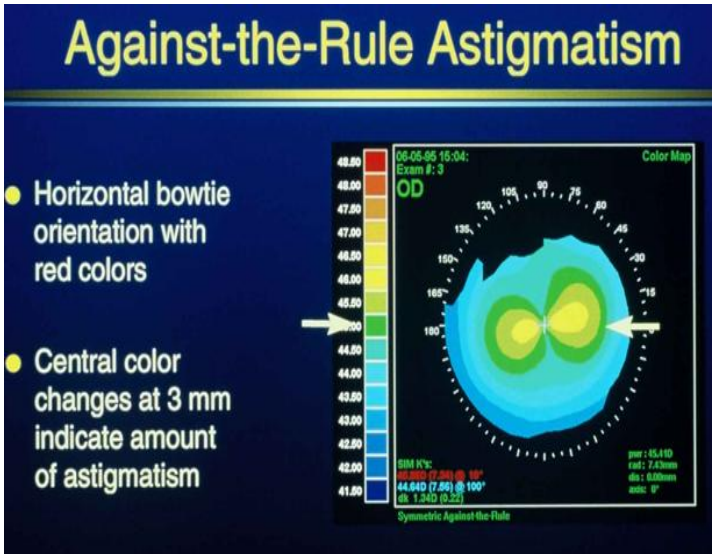


Figure 21 Against the rule astigmatic pattern

Refractive astigmatism may or may not match keratometry (or even topography). In this case almost the entire bowtie is located within the pupillary margin. That margin is a region too small for the keratometer to detect. It measures the beginning of the steepness but completely missed what would make contact lens fitting or refractive surgery planning much more difficult.

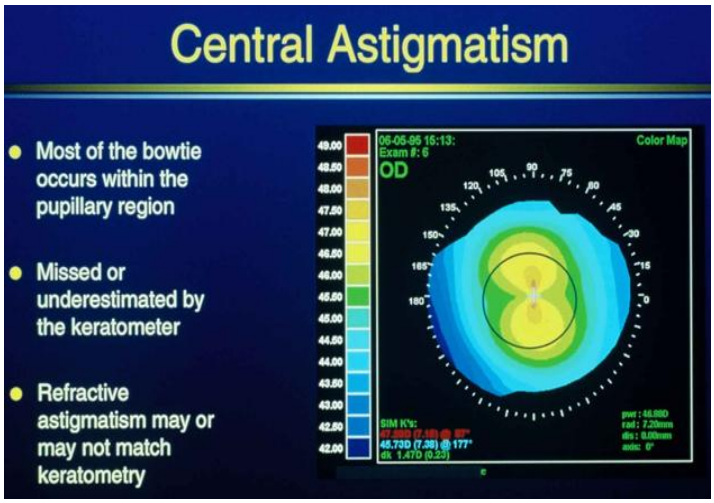


Figure 22 Central astigmatism pattern

At times the bowtie will extend all the way to the limbus. Keratometry is likely to match up with the topography as well as the refraction.

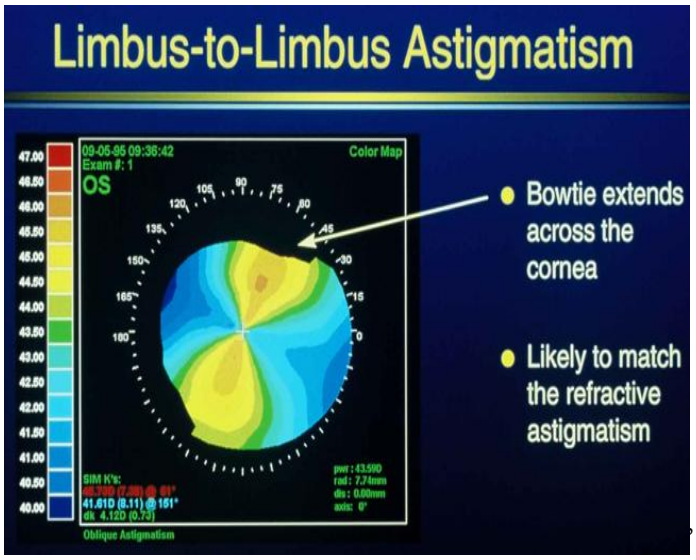


Figure 23 limbus to limbus astigmatism

If this map folded in half with the two ends of the bowtie aligned, one "bulb" would be significantly larger than the other. Where this can be significant is in refractions, refractive surgery and contact lens fitting. This cornea has multiple powers across the steeper meridian, and the patient would have to compensate for this.

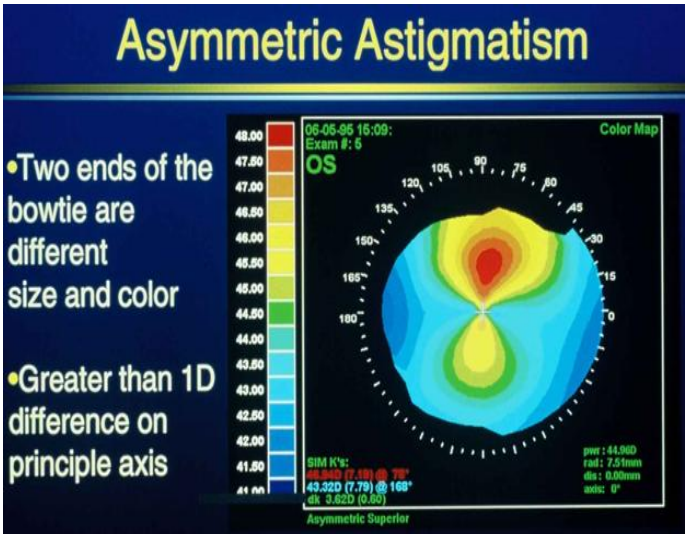


Figure 24 Asymmetric astigmatic pattern

If this map is to be folded in half, the two ends of the bowtie would not align. The principle meridians on this cornea are not 90 degrees away from each other (non-orthogonal). This patient is unlikely to see 20/20 with conventional spectacles because, again our cylindrical lenses have 2 perpendicular meridians of even power distribution. In this case, the contact lens fitter would not select a soft toric lens and the refractive surgeon would shift the astigmatic incisions to “unbend the bowtie”.

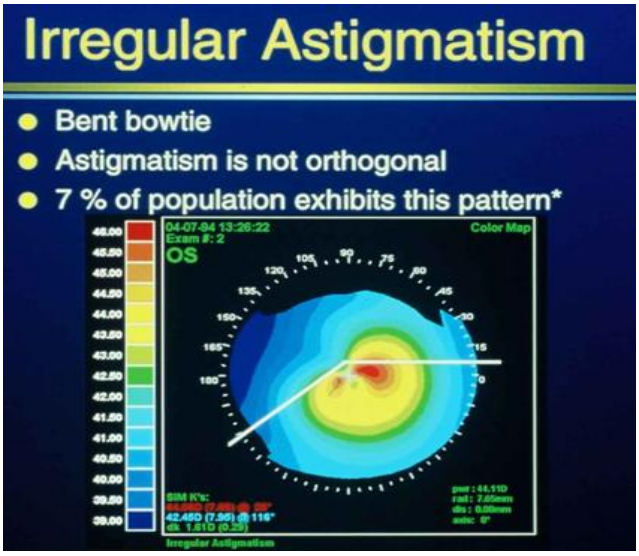


Figure 25 Irregular astigmatic pattern

## 3.3 Keratoconus diagnosis

Keratoconus is a progressive corneal disease characterized by central thinning and steepening of the corneal curvature. Keratoconus considered as a curious condition in which the central part of the cornea, begins to bulge and protrude forward as a cone. This is caused mechanically by thinning of the corneal front surface and increasing of the internal eye pressure simultaneously.

The only symptom is deterioration of vision due to irregular astigmatism caused by the changing corneal curvature. The progressive nature of this disease leads to increased myopia and irregular corneal astigmatism, which decrease visual acuity and visual quality. The following shapes show the ideal keratoconic topographic patterns.

In the beginning of Corneal Topography a significant amount of "hype" resulted in the early detection of Keratoconus. Here is a patient with clear cut keratoconus and clinical signs as well as marked topography.

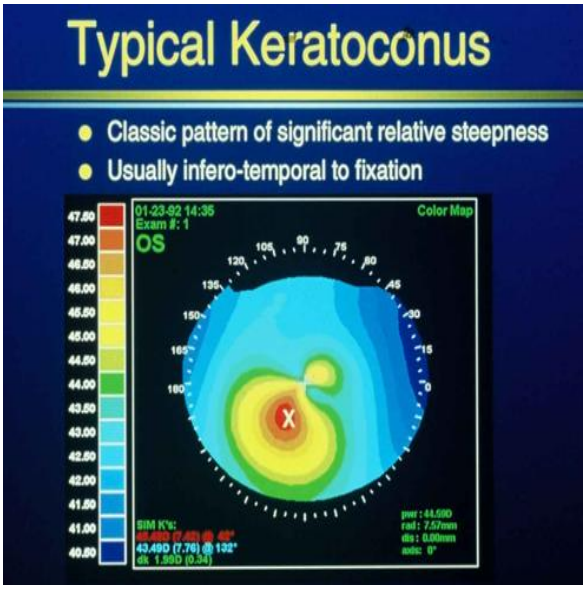


Figure 26 Typical Keratoconus

Keratoconus can also appear in unusual places. This is superior keratoconus; although superior keratoconus is rare, it is not unheard of. The range is from 53.5 – 74.5 diopters. Delta K is 18.25 diopters. Cursor is positioned at a place that measures 76.5 diopters

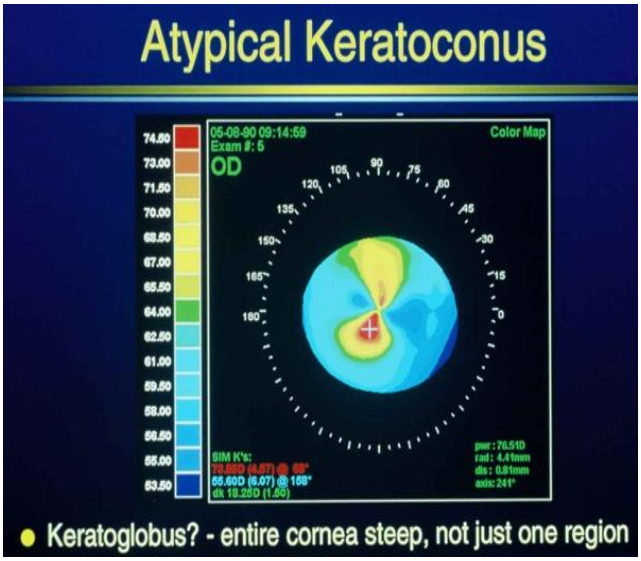


Figure 27 Atypical keratoconic pattern

# CHAPTER 4
# METHODOLOGY

## 4.1 Objective of the algorithm

Astigmatic corneas are treated with refractive surgeries (LASEK, LASIK or PRK); while Keratoconic corneas are treated with totally different procedures (Mayo-ring, Riboflavin UVA- induced cross linking Or Collagen Cross linking). Oculists make the final decision on diagnosing Keratoconus manually by interpreting data of axial and elevation maps. Since the symptoms are similar in Astigmatism also. It is necessary to differentiate these two disorders in the beginning, so that the proper treatment can be followed for the patient. In this paper an algorithm is presented to differentiate the Astigmatism from Keratoconus using Axial Topographic images. Aim of this algorithm is to suggest a computerized technique to help making this decision

1. Shape recognition mechanism.

2. Alignment recognition mechanism.

3. Pixel value access.

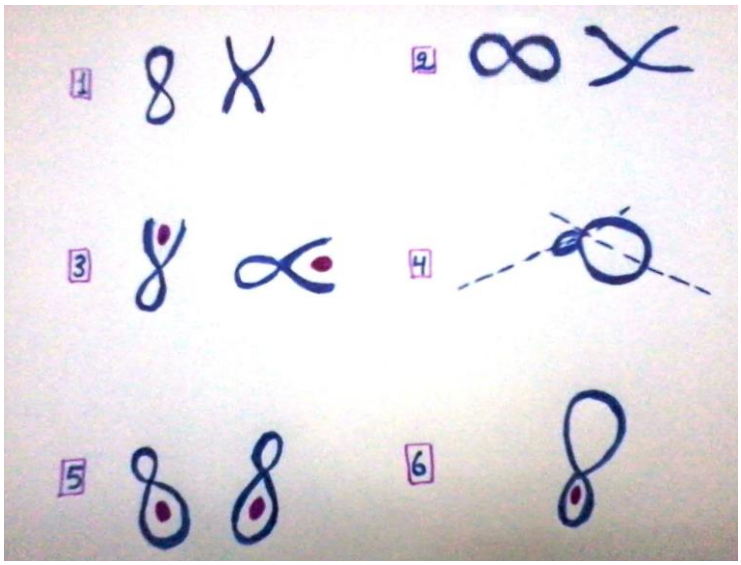


Figure 28 Bowtie shapes: (1) vertical Alignment, (2): horizontal Alignment, (3): Asymmetric bowties, (4): Not Orthogonal Axis, (5): Asymmetric slightly incline, (6) Asymmetric with smaller tie below.

## 4.2 The Algorithm

**Step 1:** Input the topographic image.

**Step 2:** Apply shape recognition algorithm to identify the bowties in the image.

**Step 3:** If the bowtie shape found fits to shape (1), or (2) (single closed end or extended shape); apply alignment recognition algorithm to identify the axis of both of the bowties.

**Step 4:** Access the pixel and assign them to diopter vales to calculate the maximum & minimum diopter in the map.

According to shape, alignment & pixel values found combinations return one of the next diagnostic results:

1-“Typical astigmatism”:(with the rule), in case of extended bowties shape, add “limbus-to-limbus”.

2-“Typical against the rule astigmatism”. In case of extended bowties shape, add “limbus-to-limbus”.

3- Asymmetric astigmatism, here the higher valued diopter should be inside the closed loop regardless of the alignment.

4-In case of not orthogonal axis, return the result: “Irregular Astigmatism”.

5-In case of closed loop shape with an alignment of -30degrees to 30 degrees vertical alignment& higher diopter values inside the lower loop return the result “Typical keratoconus”.

6- Same in last case but vertically flopped shape return the result “Atypical keratoconus”

## 4.3 Methods for the proposed algorithm

### 4.3.1 Input Data

All the samples are for patients of Dr.G.S Randhawa Eye Hospital. Data base is a selected group of (151) PETACAM images for suspicious astigmatic and keratoconic eyes. The Region Of Interest (ROI) in the input image is the axial front map, this portion is only used for the purpose of classification as shown in figure.

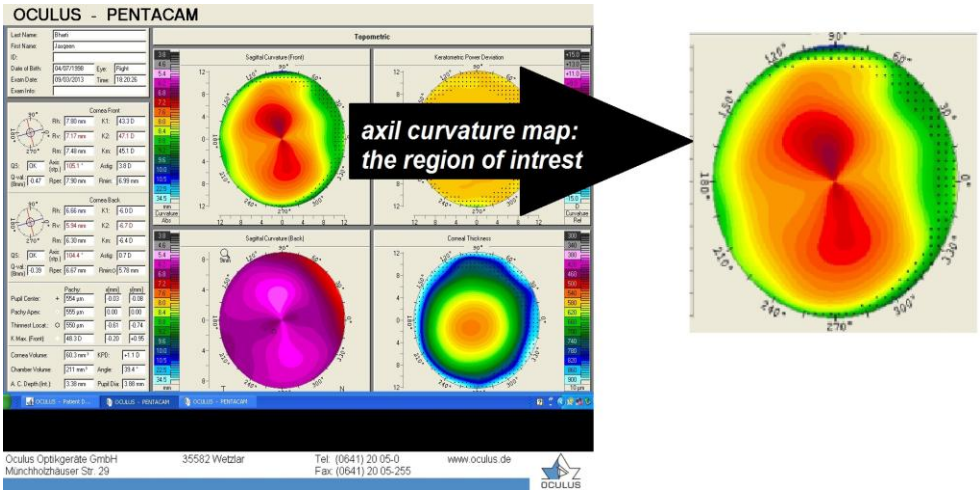


Figure 29 Region of interest in the input image.

### 4.3.2 Testing the behaviour of the images

All the image processing techniques can be done in greyscale level; no lose of data occurred while converting from RGB to Grey & even to B&W.

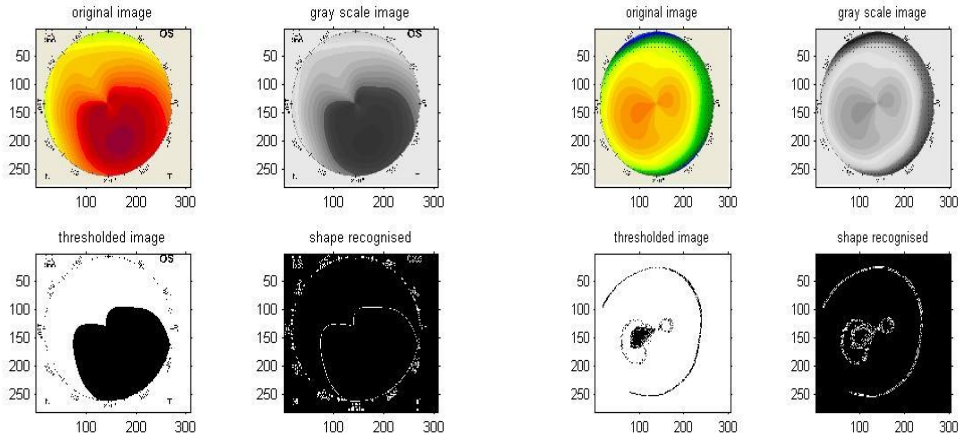


Figure 30 Topographic patterns are not affected by converting the input image from level to another. (A) Keratoconic eye, (B): Astigmatic eye.

### 4.3.3 Thresholding

Some global thresholding methods like Otsu method and adaptive methods also like local contrast method were applied to define a thresholding method while extracting the patterns. (Converting from greyscale to black and white). Both of these two methods didn't show good response for all the images. Global thresholding methods were not able to extract the shapes properly and extra noise was there for all the images, while adaptive method was not able to extract the shapes effectively (fully). This is due to the fact that the same topographic representation can be represented with totally different colour and hence greyscale images; (with the aid of scales as presented by corneal topographers). Every image has its own unique response to the known thresholding techniques; for that the thresholding method used to extract the topographic method has been established after number of experiments; in this algorithm each single image is thresholded adaptively by selecting a pixel value from the boundary region of the colour image using the command "ginput" as shown in figure below.

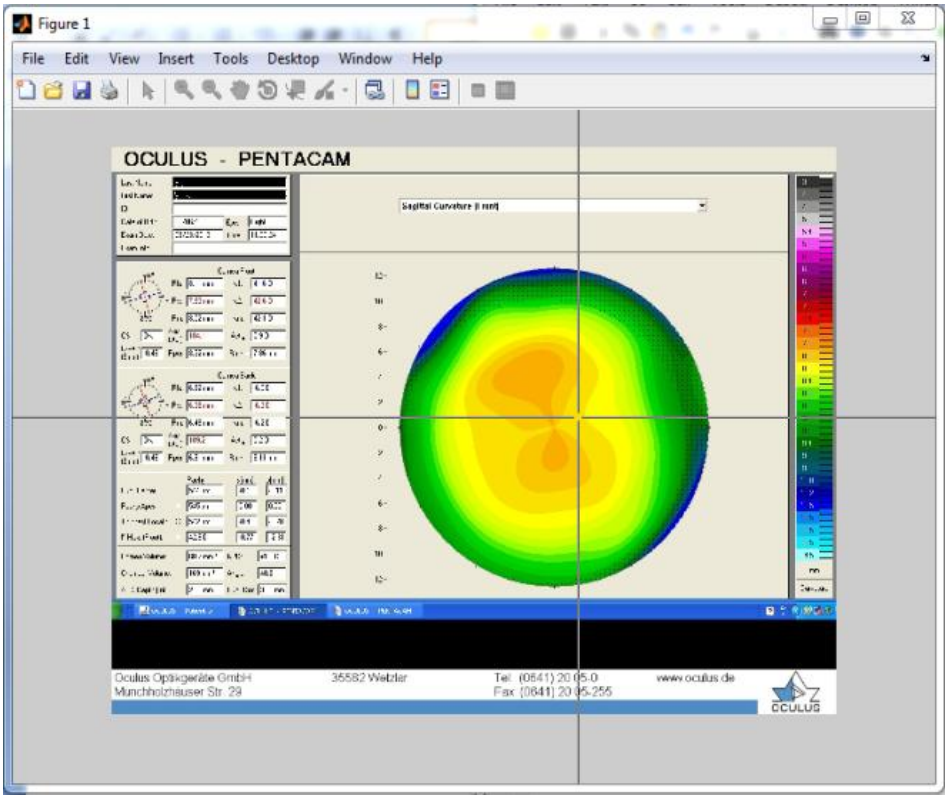


Figure 31 Thresholding step using ginput command.

### 4.3.4 Logical & Morphological Operations

Randomly logical and morphological operations have been applied to the images to get prior impression on their behaviour. After certain tests, some morphological operations have been selected as the classification operators for the input images.

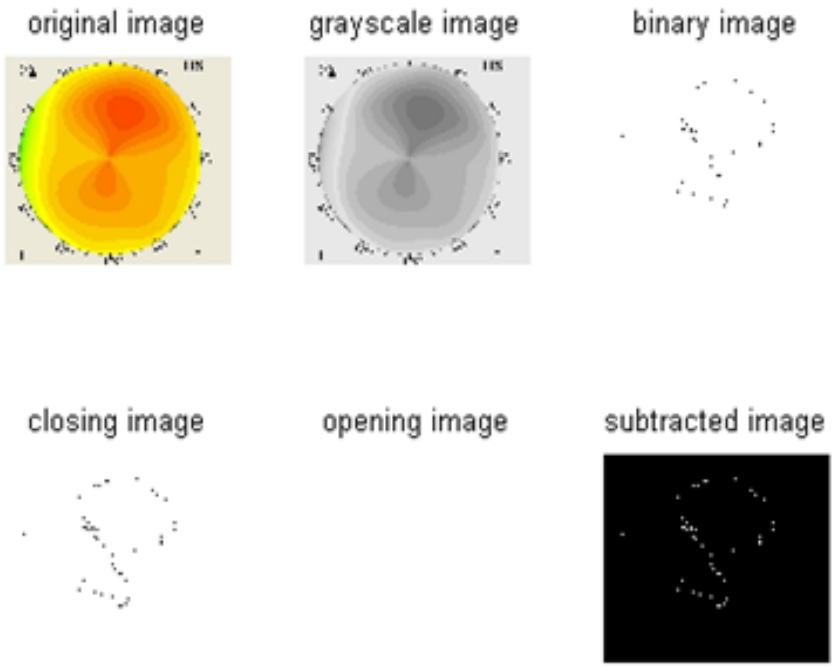


(A)

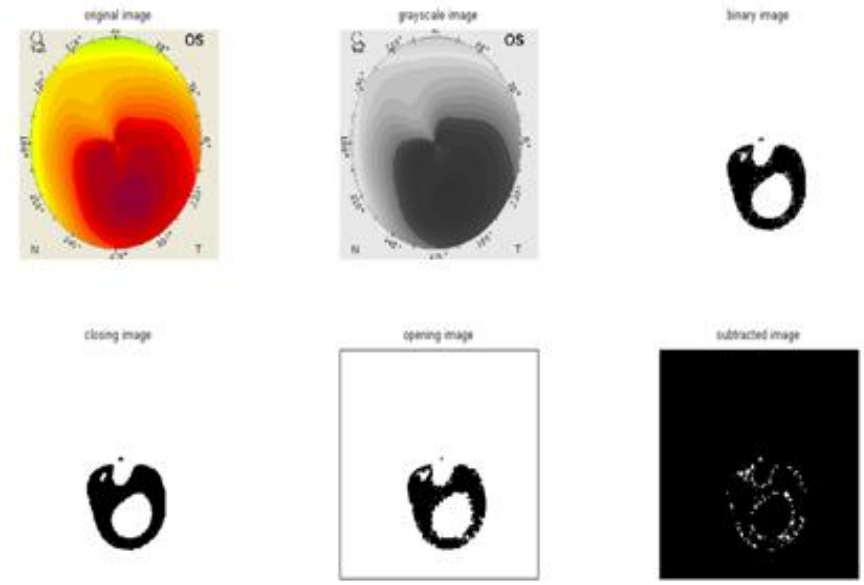


(B)

Figure 32 Random testing: (A); astigmatic eye, (B) Keratoconic eye.

### 4.3.5 Tests

#### 4.3.5.1 Test no.1:

***Objective:***

To examine the effect of every "basic" morphological operation separately on all the images.

***Number of Morphological Operations:***

Seven; erode, dilate, open, close, thin, thick & skeleton.

***Conclusion:***

***1)*** Individual comment on "*Image response* vs. *Diagnoses*" for every image has been recorded for the next experiments.

***2)*** The foreground (black) & background (white) of the images should be swapped in the binary image; to get better results.

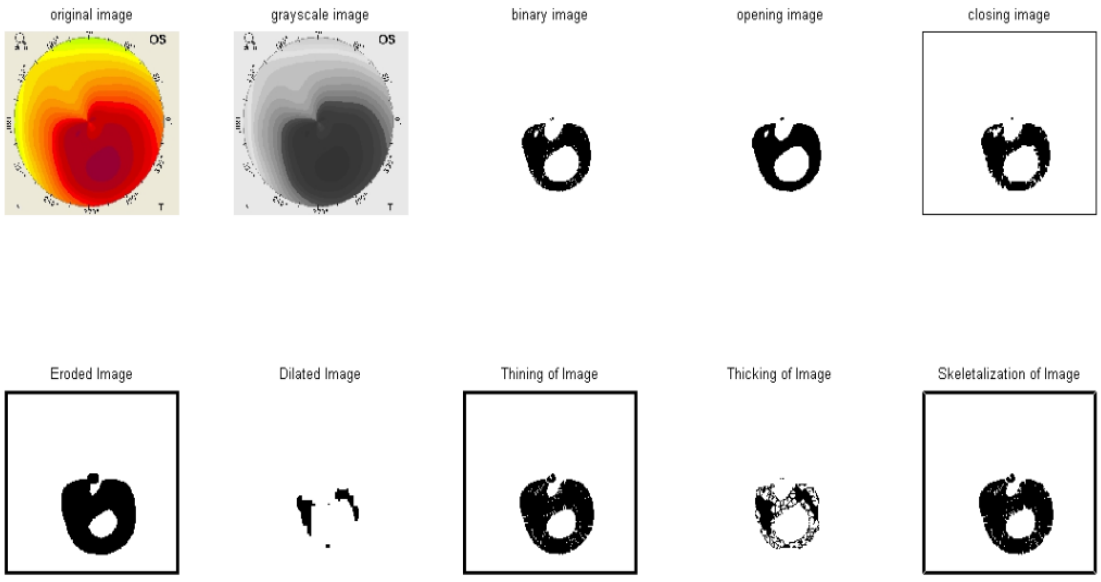


Figure 33: Test (1): (a): Image No (2): keratoconic eye response.

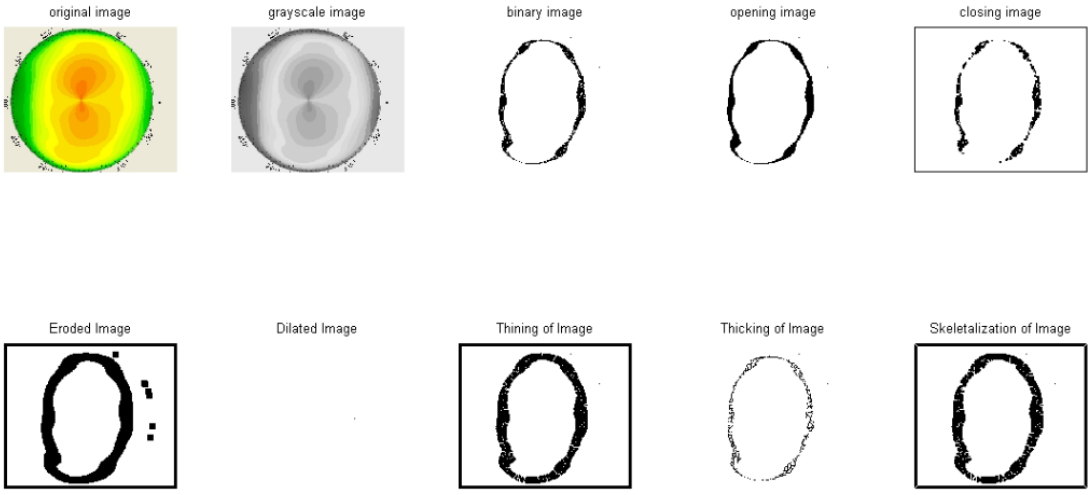


Figure 34 Test (1): (b): Image (9): Astigmatic eye response.

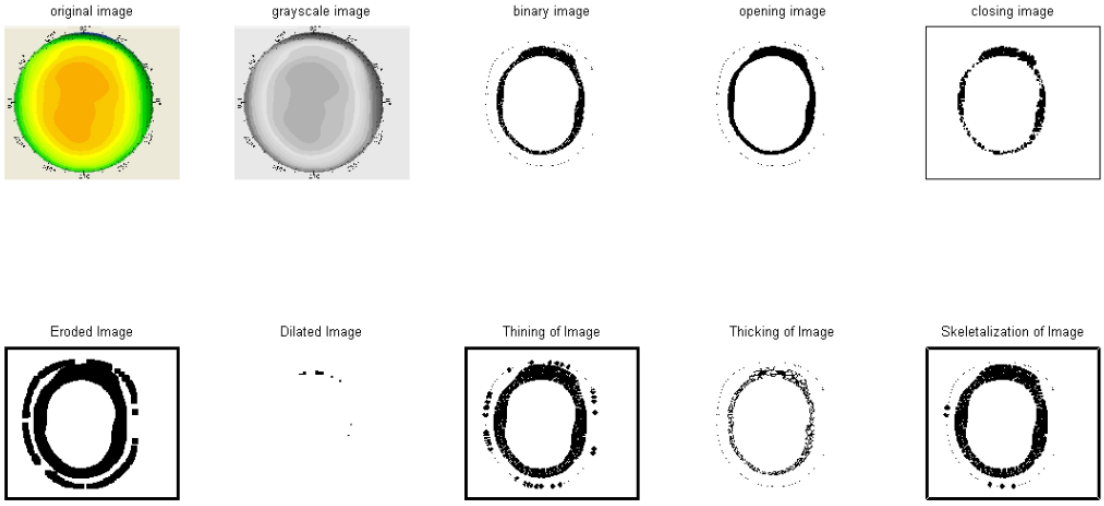


Figure 35  Test (1): (c): Image (26): Normal eye response.

#### 4.3.5.2 Test no.2:

***Objective:***

Same as in test (1) but: to include two thresholding values instead of one & adjusting the binary representation according to conclusions of test (1).

***Number of morphological Operations:***

Seven; erode, dilate, open, close, thin, thick & skeleton.

***Conclusion:***

***1)*** The number of thresholding values & combinations of Boolean relation among them has no effect on the response of the images.

***2)*** Position of the selected threshold value affects the response; for all the images: position of thresholding values are:1;anywhere on meridians & 2; anywhere on the boundary region of the (circular/ bowtie) shape

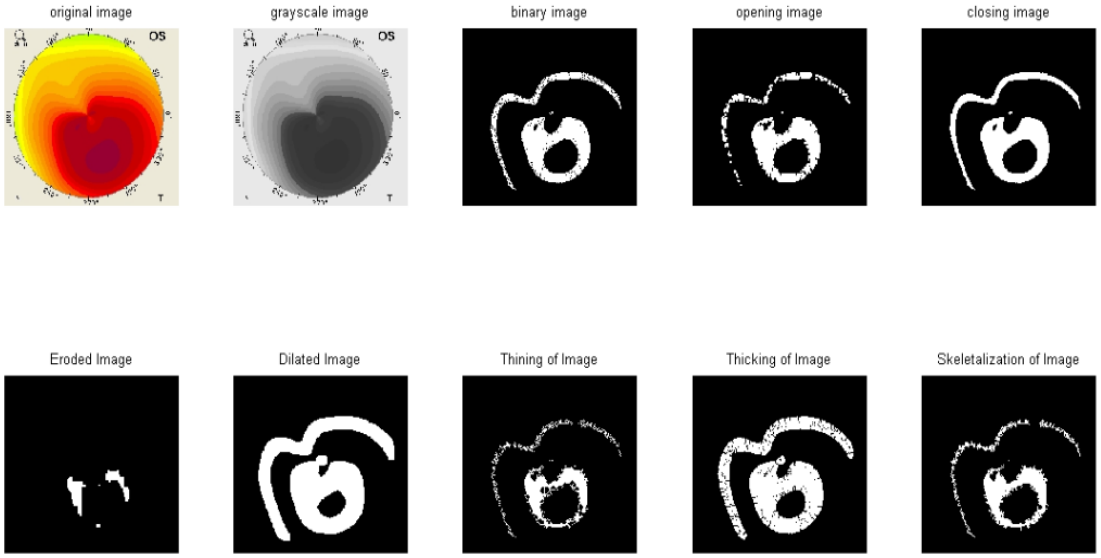


Figure 36 Test (2): (a): Image No (2): keratoconic eye response.

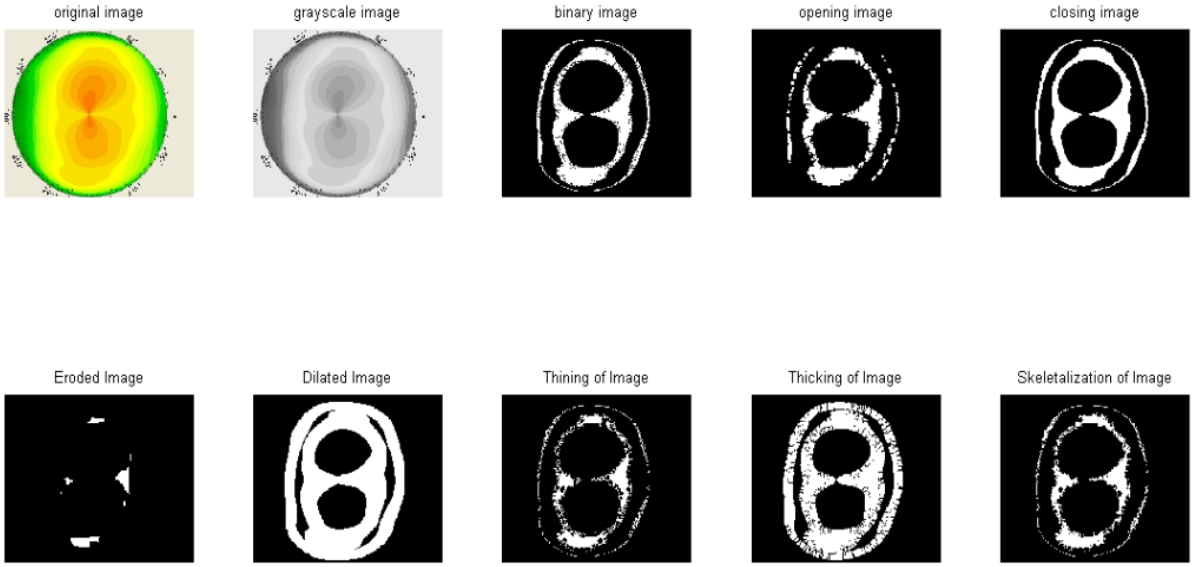


Figure 37 Test (2): (b): Image (9): Astigmatic eye response.

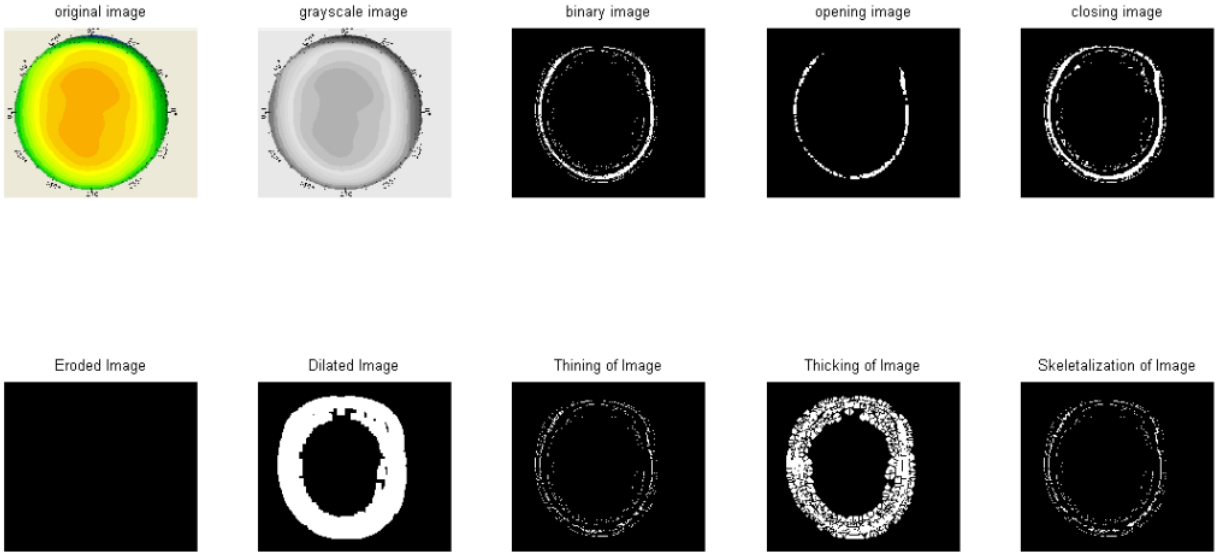


Figure 38  Test (2): (c): Image (26): Normal eye response.

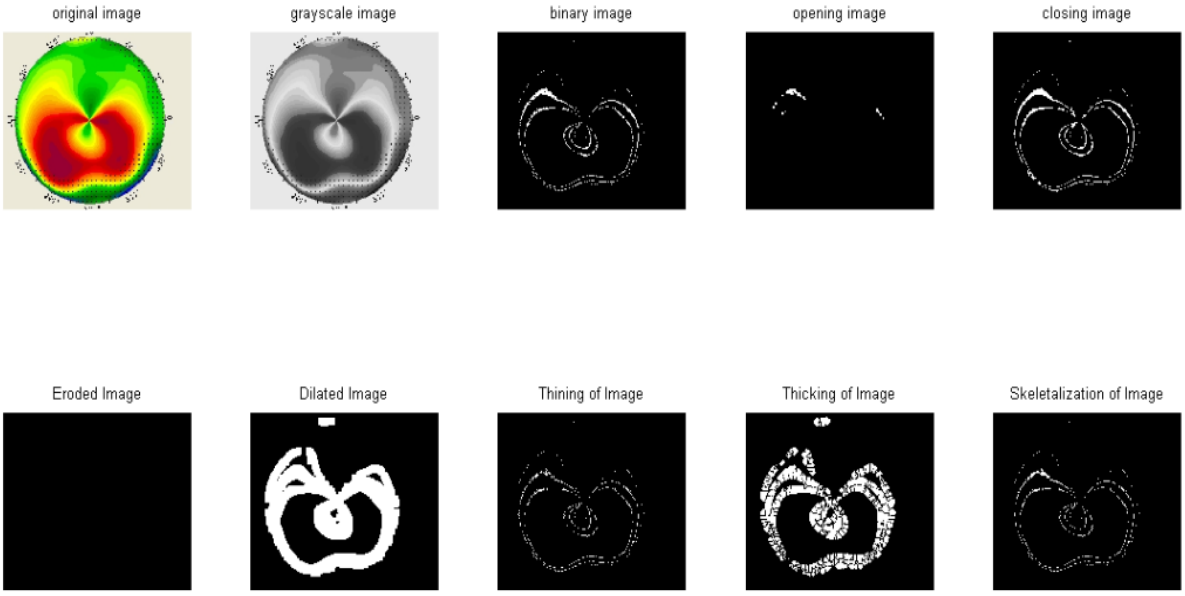


Figure 39 Test (2): (d): Image (41): Another normal eye response.

#### 4.3.5.3 Test no.3:

***Objective:*** *Same as in test (2)* but: to find out the best neighbourhood index for each morphological operation & eliminating the test morphological operation for the next experiment.

***Number of morphological Operations:***

Seven; erode, dilate, open, close, thin, thick & skeleton.

***Conclusion:***

***1)*** Dilating at 5-7 pixels and closing at 10-20 gave the finest results for all images.

***2)*** Dilating, closing and skeletonising are elected for the next experiment.

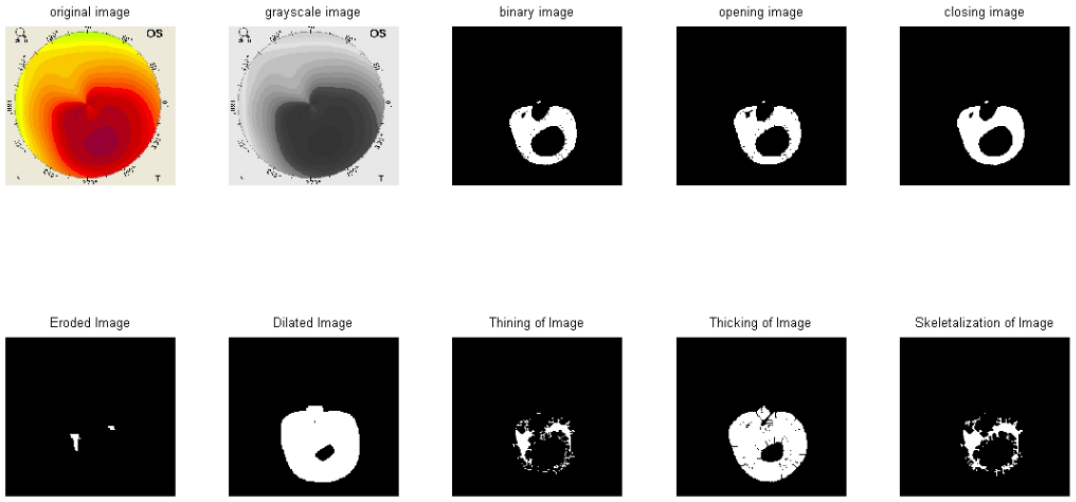


Figure 40 Test (3): (a): Image No (2): keratoconic eye response.

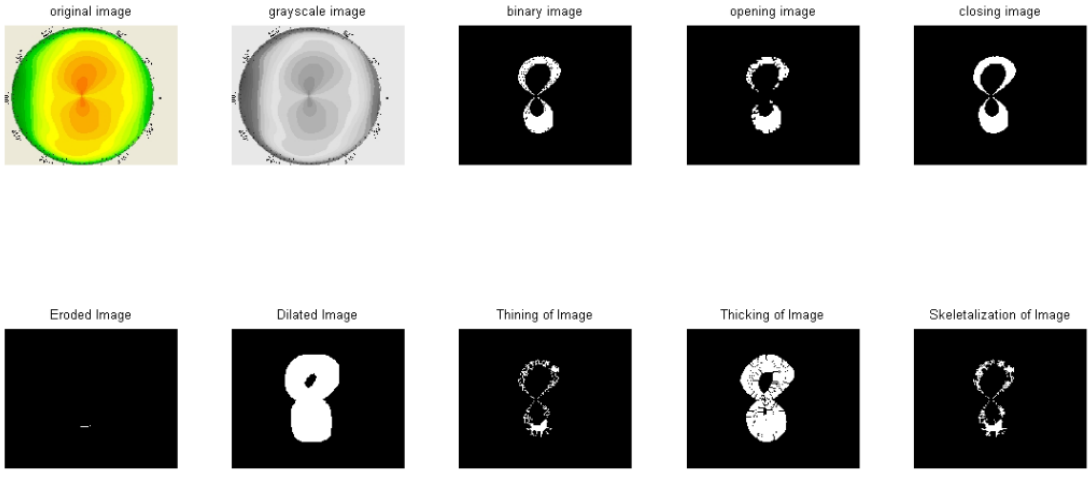


Figure 41 Test (3): (b): Image (9): Astigmatic eye response.

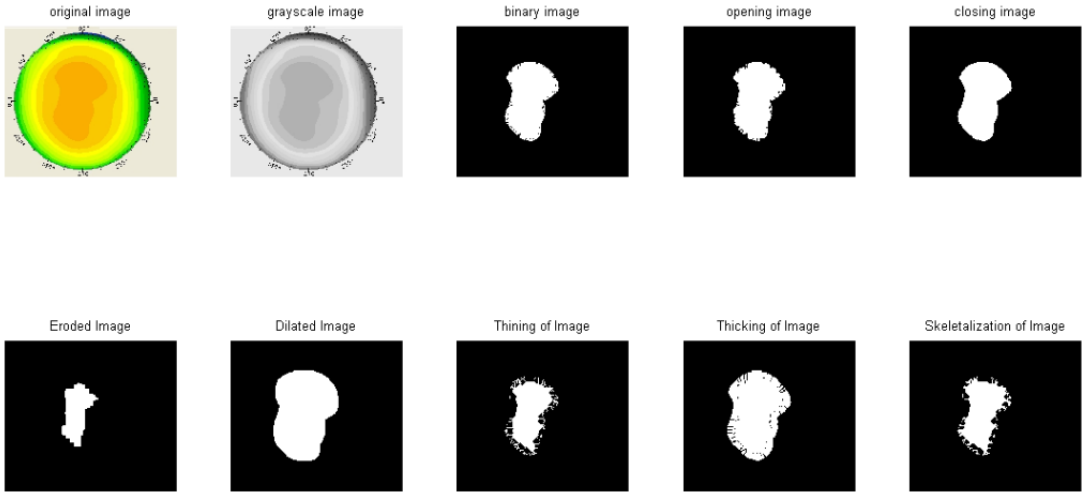


Figure 42  Test (3): (c): Image (26): Normal eye response.

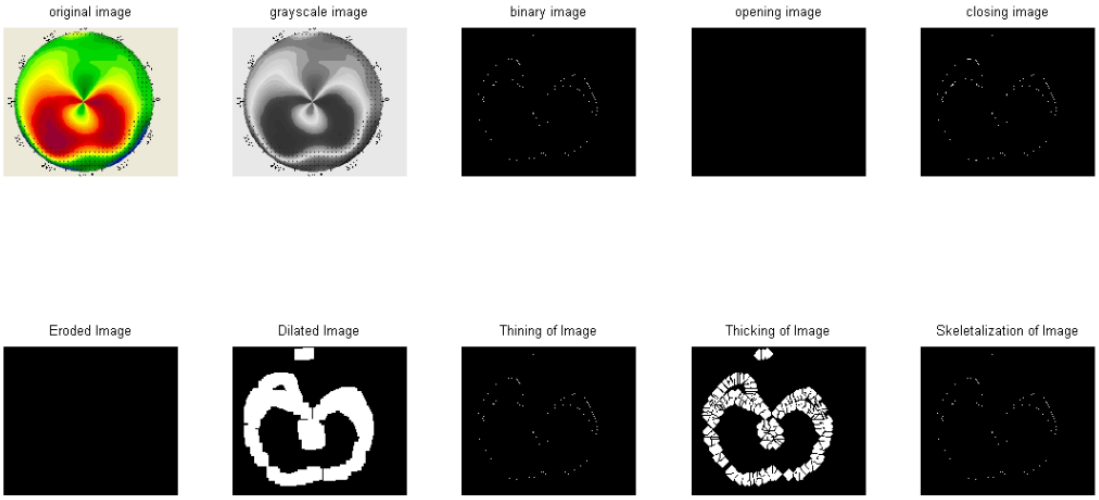


Figure 43 Test (3): (d): Image (41): Another normal eye response.

#### 4.3.5.4 Test no.4:

***Objective:***

To examine the effect of closing and dilating and choosing the best neighbourhood for each one.

***Number of morphological Operations:***

Two; dilate, & close.

***Conclusion:***

The best morphological operation in refining the topographic pattern is closing.

The best neighbourhood value is 25 pixel, till no change occurs is the enhancement technique chosen to refine the images.

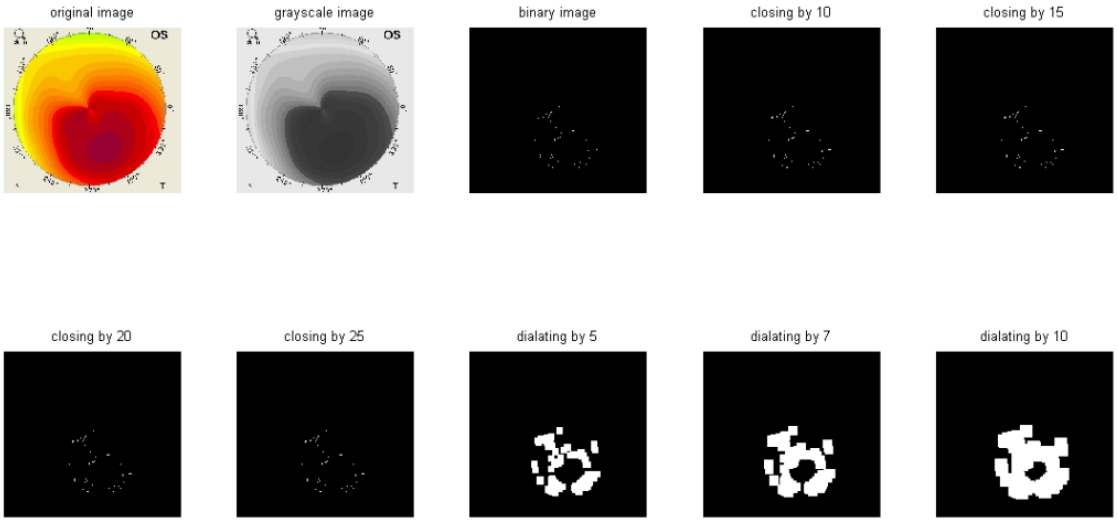


Figure 44 Test (4): (a): Image No (2): keratoconic eye response.

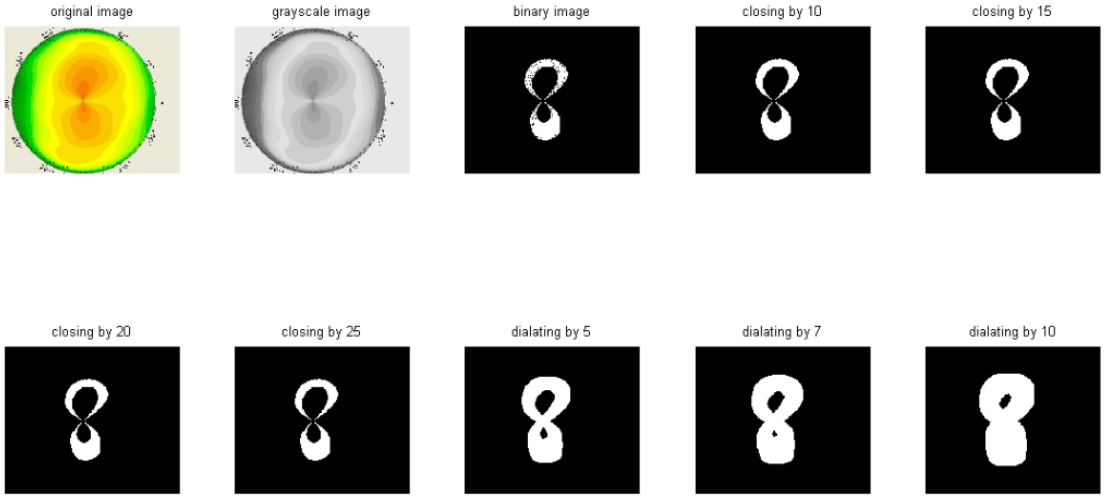


Figure 45 Test (4): (b): Image (9): Astigmatic eye response.

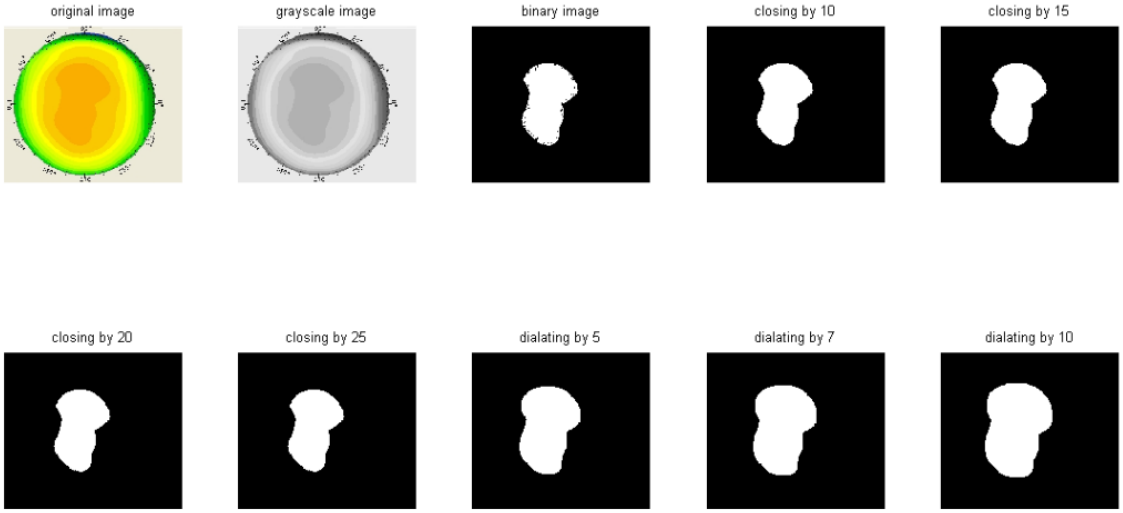


Figure 46  Test (4): (c): Image (26): Normal eye response.

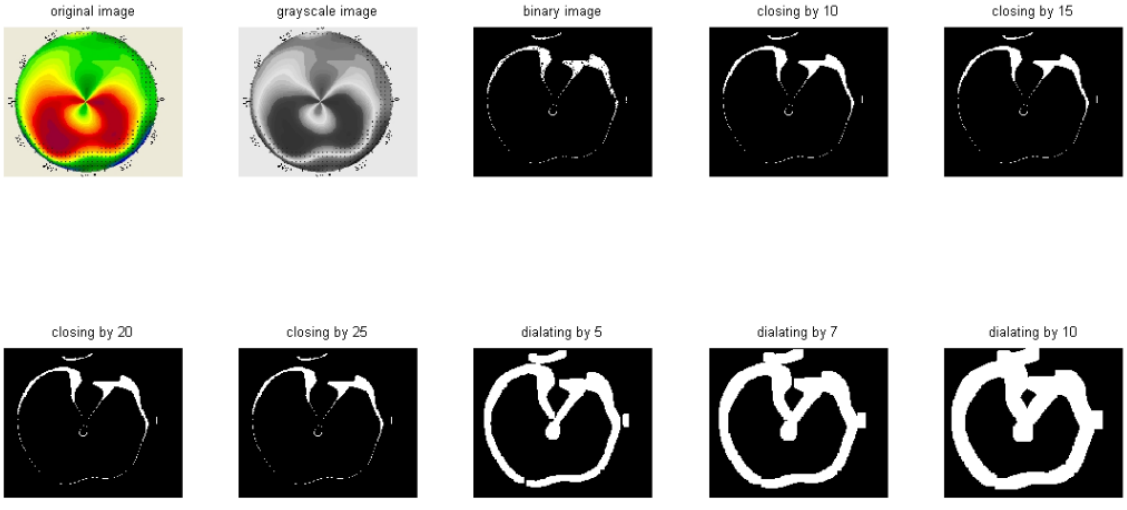


Figure 47 Test (4): (d): Image (41): Another normal eye response.

#### 4.3.5.5 Test no.5:

***Objective:***

To examine the effect of closing at 25, dilating at 5 & 7 and skeletonising at 5and choosing the best neighbourhood for each.

***Number of morphological Operations:***

Three; dilate, close & skeleton.

***Conclusion:***

Closing at 25 is the best; it refines the detected patterns better than any combinations of morphological operations.

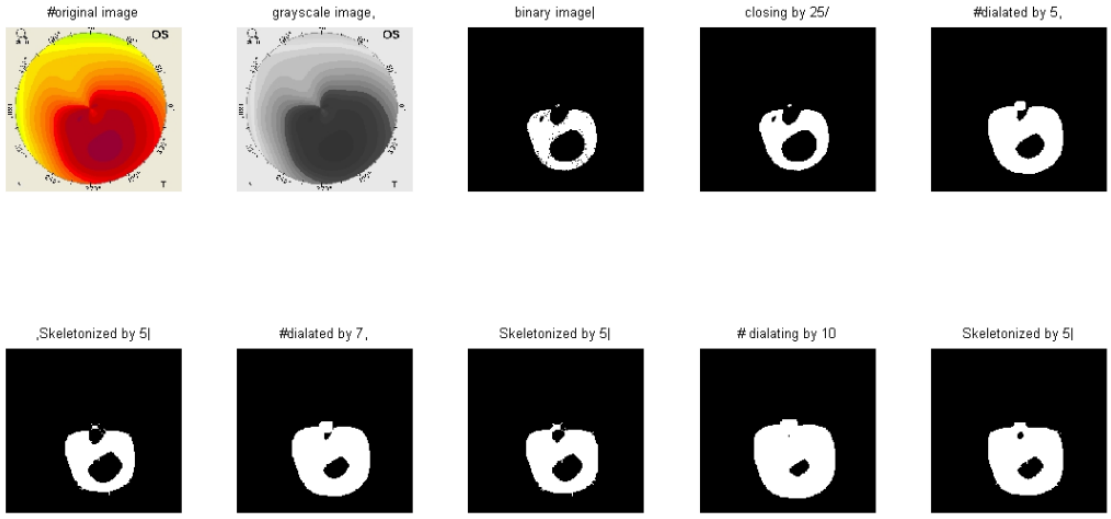


Figure 48 Test (5): (a): Image No (2): keratoconic eye response.

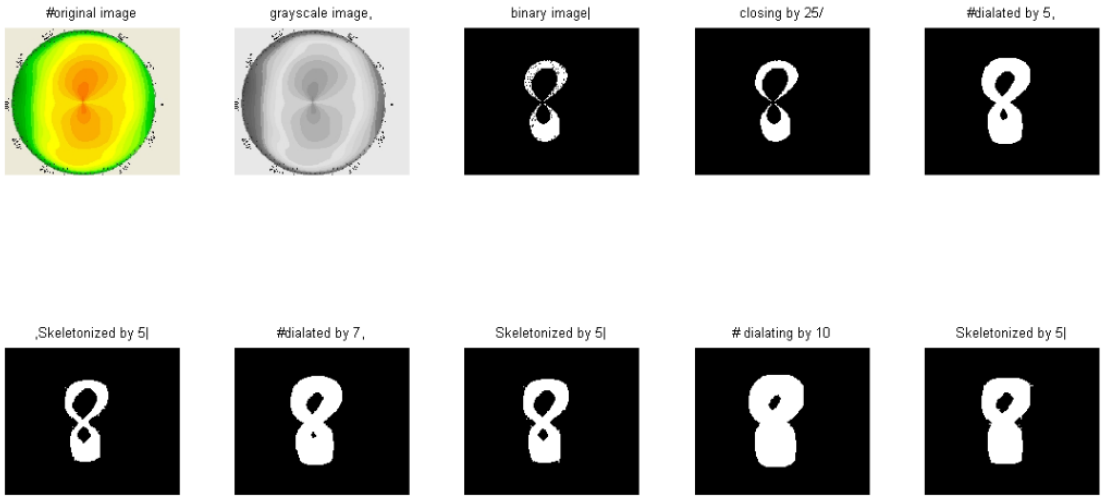


Figure 49 Test (5): (b): Image (9): Astigmatic eye response.

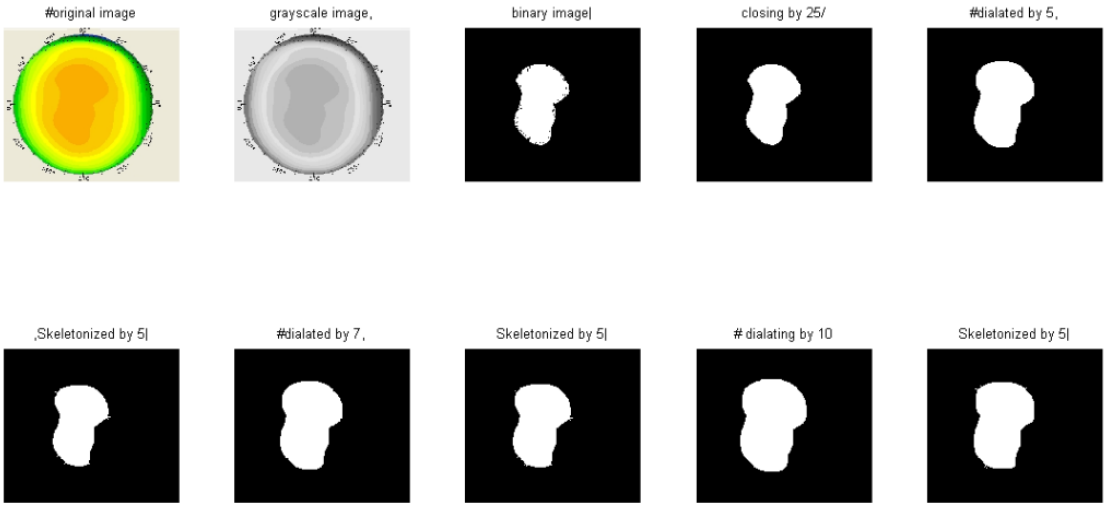


Figure 50  Test (5): (c): Image (26): Normal eye response.

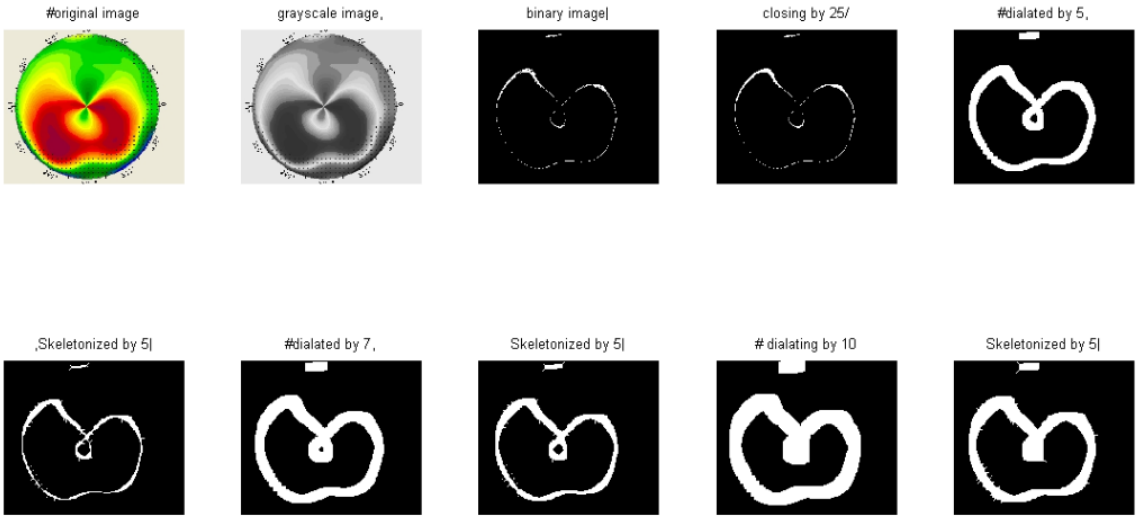


Figure 51 Test (5): (d): Image (41): Another normal eye response.

At this point of testing response of the images got better sufficiently; so no need to perform more tests. The next step in methodology applied is shape matching

### 4.3.6 Shape matching

Cross correlation is used to determine the similarity between the ideal patterns of each disease and the input image. Alignment is automatically included by using orthogonal shapes. The following figure shows the astigmatic shapes found in literature; from which the matching default shapes were extracted to diagnose astigmatism.

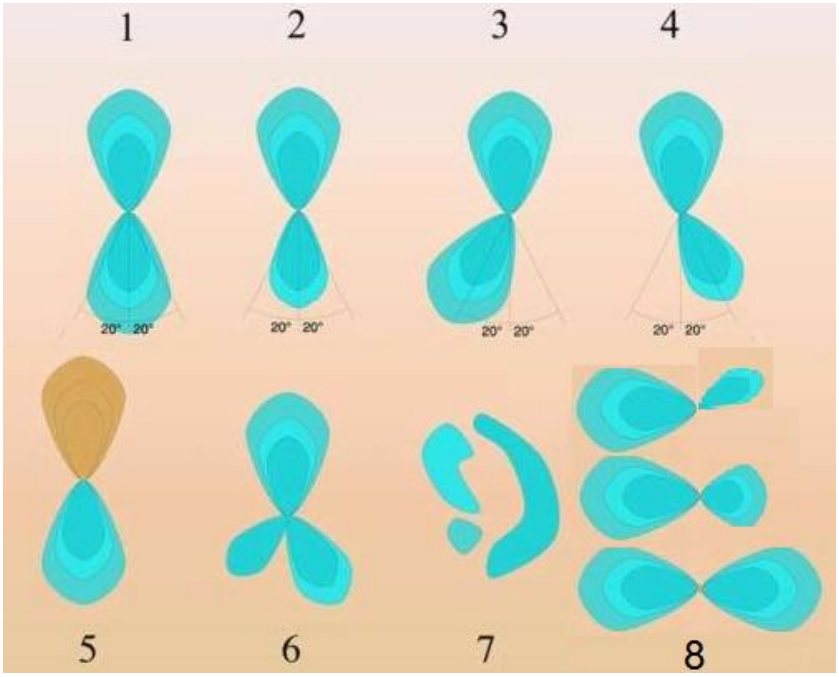


Figure 52 The shapes used for auto and cross-correlation operations: 1&2 are with the rule astigmatism orthogonal symmetric, 2&3 are with the rule non-orthogonal symmetric,5 is keratoconus-like ( with the rule astigmatism), 6 is poly-axigonal (immeasurable), 7 is the irregular astigmatism, and 8 is for the "against the rule astigmatism" cases.

The following figure shows the default shapes used in MATLAB program to determine cross correlation values on which type of astigmatism classification was decided.

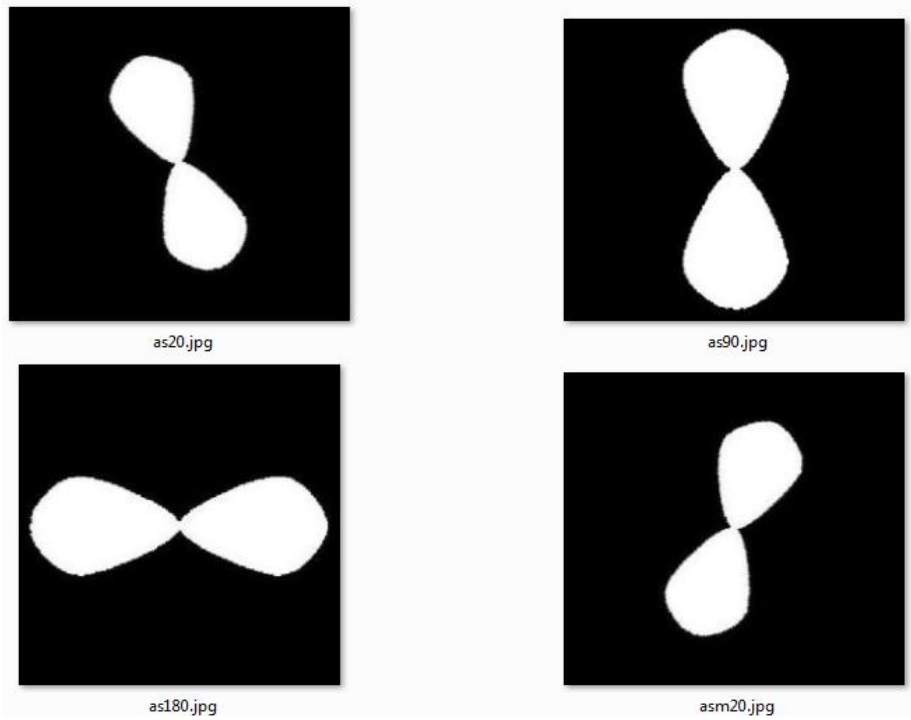


Figure 53 Types of Astigmatism defualt matching shapes used in MATLAB program.

After RGB to gray conversion, thresholding and morphological operations the topographic patterns of normal eyes will appear just like a big round shape centered in center of the map, while the keratoconic eye will tend to have smaller round shape placed at the middle or slightly incline lower half of the map. This phenomenon doesn't has any contrast with definition and characteristics of the disease in ophthalmology references'. Default shapes were selected to determine cross correlation values on which normal eyes and keratoconus and classification was decided. It is clear that

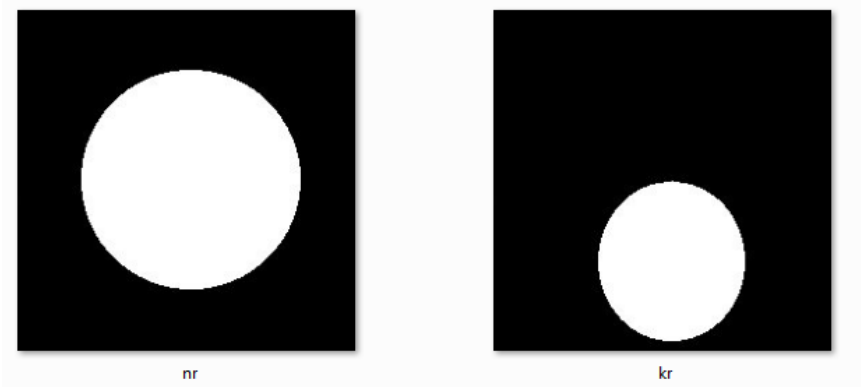


Figure 54 Keratoconus default matching shape used in MATLAB program.

# CHAPTER 5
# RESULTS AND DISCUSION

## 5.1 Performance comparison

To evaluate the diagnostic method (test), the sensitivity and specificity analysis is used [43]. To emphasize the significance of feature fusion, the classification verified by the expert eye specialist for each test image and then TP, TN, FP and FN are found and the *confusion matrix* is shown in Table 2.

Table 2 Confusion matrix

| | Predicted P | Predicted N |
|---|---|---|
| Actual P | True Positive | False Positive |
| Actual N | False negative | True Negative |

After running the MATLAB program based on the proposed algorithm; the results of 111 images out of 150 images met the actual diagnosis provided by the eye specialist; distributed as 87 and 24 for TP and TN respectively; While 39 of them missed the actual diagnosis; distributed as 26 and 12 for FP and FN respectively as shown by the confusion matrix below.

Table 3 Result in the Confusion matrix

| | **P** | **N** |
|---|---|---|
| **P** | **87** | **27** |
| **N** | **12** | **24** |

It is obvious from this distribution of results over the confusion matrix that the accuracy of the proposed approach reaches the value of 74% calculated according to accuracy equation below.

$$\textbf{Accuracy} = \frac{\textbf{TP} + \textbf{TN}}{\textbf{Total samples}} * 100\%$$

## 5.2 Actual diagnosis vs. results of proposed algorithm

1) 24 images are of normal corneas and the results came ***compatibly normal as*** image number (138) shown in figure 55.

2) 41 images are for Astigmatism and the results came of ***compatibly of with the rule Astigmatism,*** as image number (79) shown in figure 56.

3) 27 images are of against the rule Astigmatism and the results came ***compatibly of against the rule Astigmatism*** as image number (30) shown in figure 57.

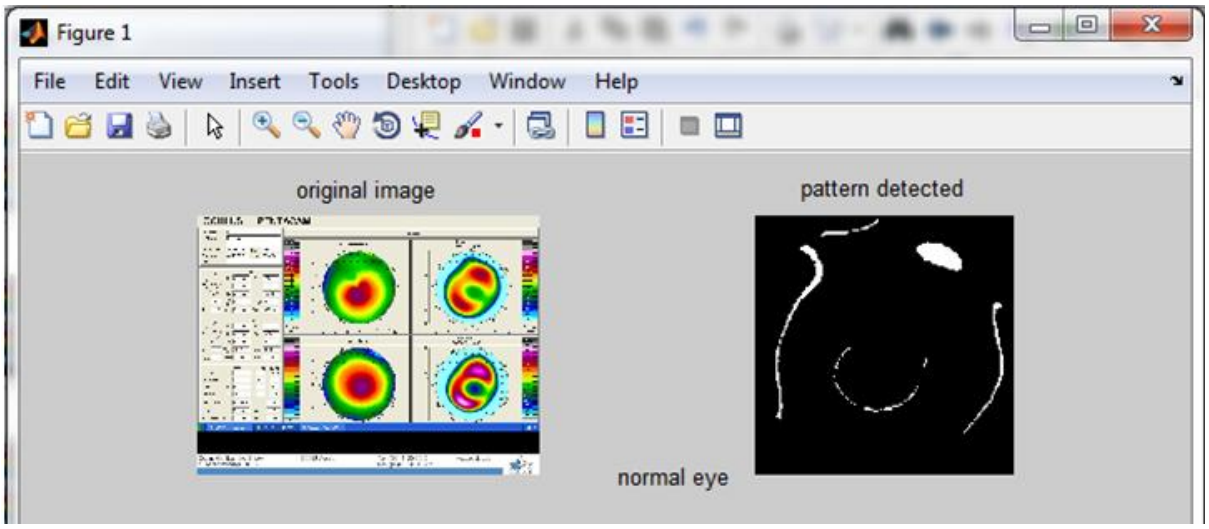


Figure 55 successfully classified normal cornea

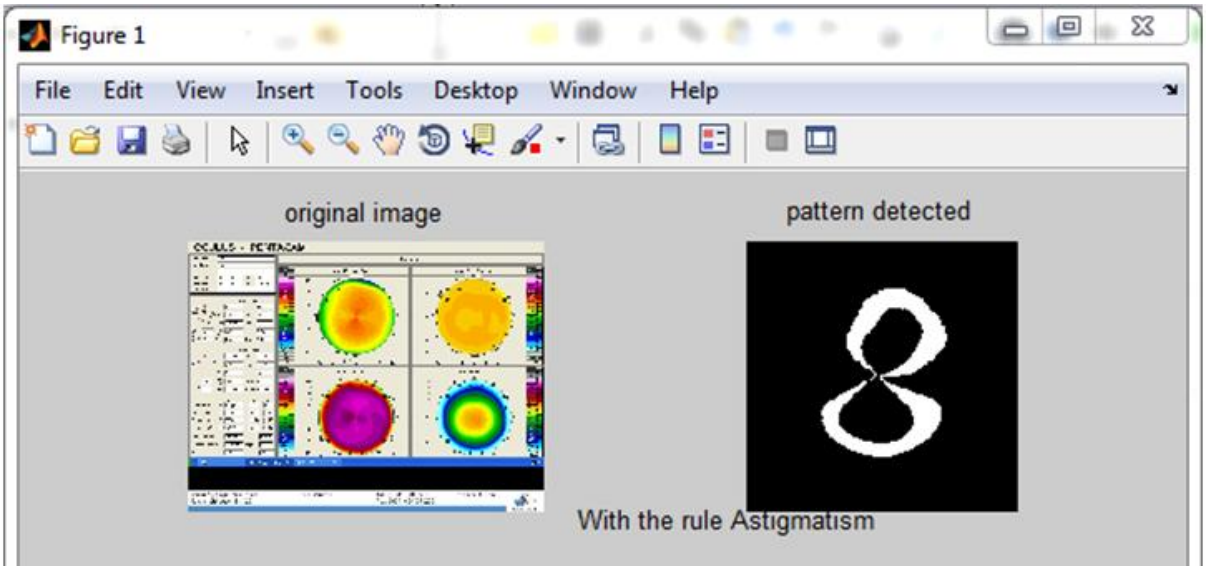


Figure 56 successfully classified Astigmatism

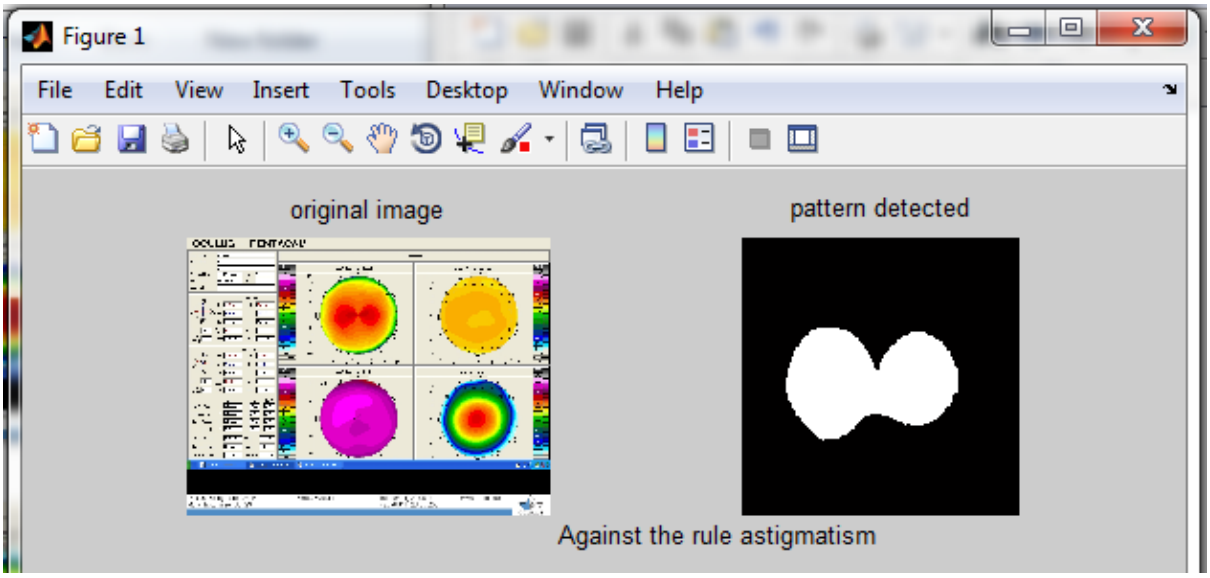


Figure 57 successfully classified Astigmatism

4) 19 images were ***successfully*** classified as keratoconic eyes like image number (146) shown in figure 58.

5) 20 images had the results of astigmatic eyes ***mistakenly*** while they belong to normal eyes. As image number (36) shown in figure 59.

6) 7 images were classified ***mistakenly*** as keratoconic eyes while they are actually normal. As image number (4) shown in figure 60.

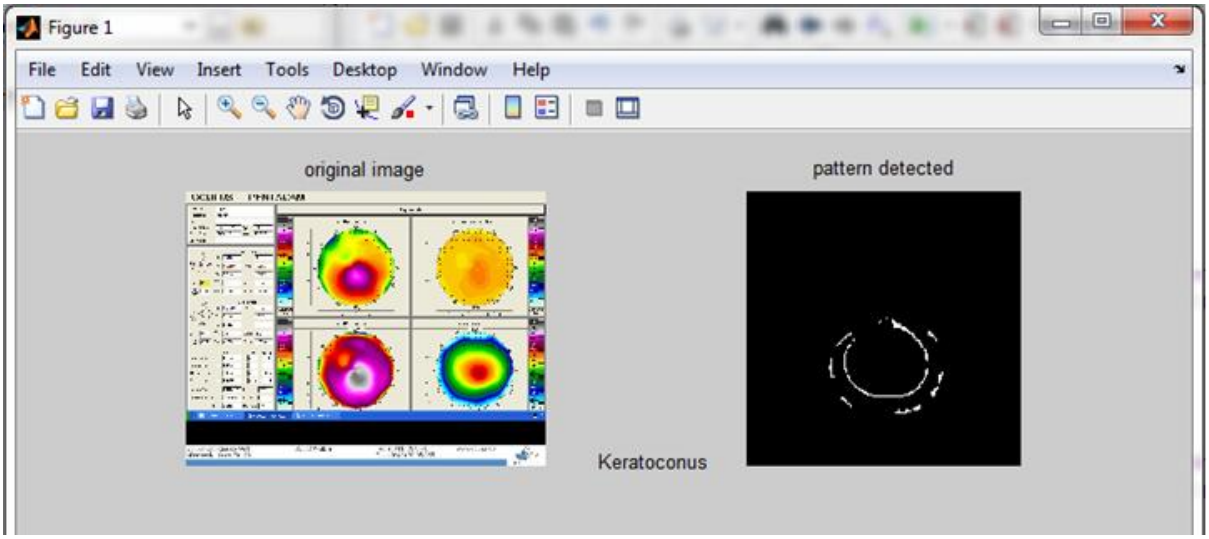


Figure 58 successfully classified as keratoconic eye

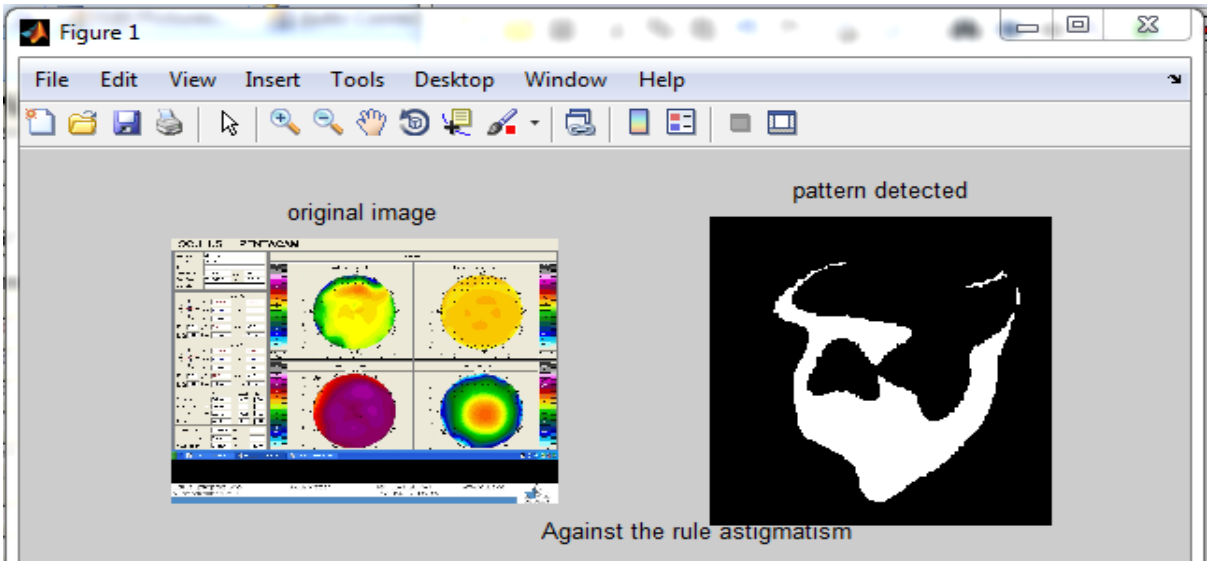


Figure 59 mistakenly classified Astigmatism

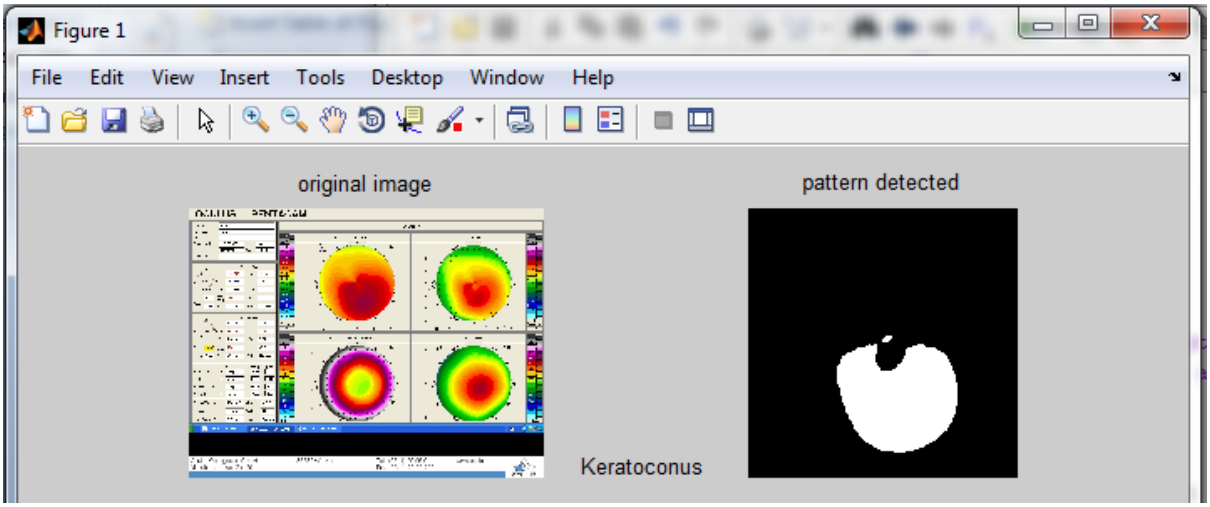


Figure 60 mistakenly classified as keratoconic eye

7) 9 images are of posterior keratoconus but the results showed ***mistakenly that they have either normal or astigmatic corneas***. The proposed algorithm failed to detect the posterior keratoconus because the input images are of anterior corneal surface only. Image number (7) was one of those cases; as shown in figure 61.

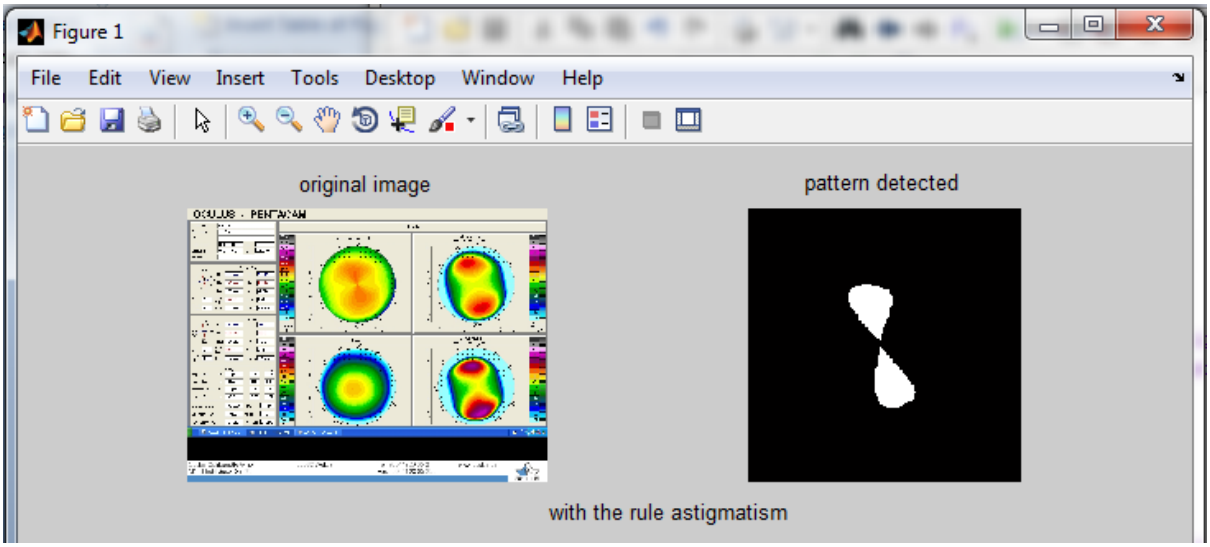


Figure 61 mistakenly classified as astigmatic eye

8) 3 images are of acute keratoconus on both anterior and posterior corneal surfaces, but again the proposed algorithm failed to detect it and showed that they have ***normal corneas mistakenly***; due to a scar placed above or nearby the apex of the cone, which affected the topographic maps as shown in figure 62 which belongs to image number (54) .

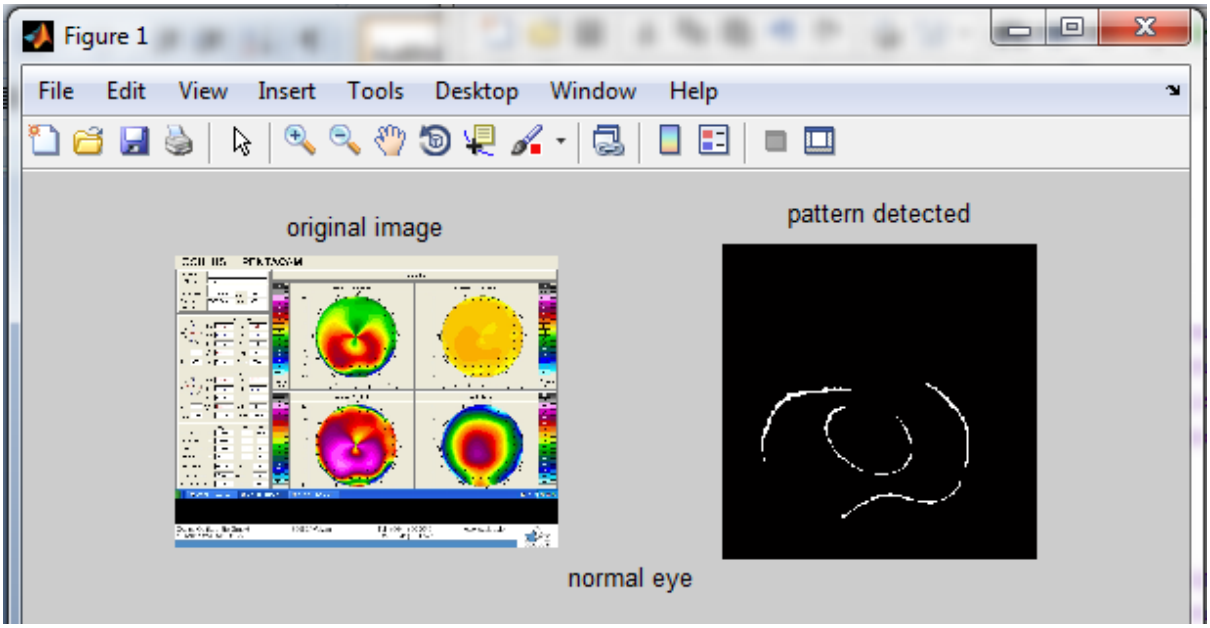


Figure 62 mistakenly classified as normal eye

## 5.3 comment on results

Axial maps (saggital curvature maps) convey the majority of the refractive corneal data, but for 100% correct results; axial maps can’t stand alone without the aid of elevation maps in diagnosing eye refractive disorders and keratometry. However; front corneal curvature could provide very good expectation while trying to differentiate between keratoconic and astigmatic eyes using the proposed algorithm.

# CHAPTER 6
# CONCLUSION AND FUTURE SCOPE

## 6.1 Conclusion

From results and discussion it has been concluded that the proposed algorithm presented an efficient approach to differentiate Keratoconic from Astigmatic corneal eyes successfully by a ratio of 74 % applying it to PENTACAM axial front corneal maps.

New method of thresholding was presented which is not governed by any mathematical restriction; its thresholding value is a costume pixel value driven from a user defined click. This provides more flexibility while dealing with the unique PENTACAM images.

Number of morphological operations has been selected and combined in testing procedure to find a suitable enhancing method for the purpose of extracting the topographic patterns.

The classification step is based on similarity measure determined by comparison of cross-correlation factors between the detected pattern and a number of default (ideal) pattern for each case. The final result of every image is the associate default shape for the maximum cross-correlation factor among all.
The total number of selected images was 150; all of them are candidates for refractive surgery with either suspect keratoconic eyes or eyes with refractive errors as well as a presence of keratoconic suspicion, this algorithm succeeded in making the right decision for 111 of them.

## 6.2 Future Scope

Since refractive surgery is based on the concept of reshaping or the cornea to meet the normal eye curvature (filing or rasping its surface) the surgeon has to make sure that the eye is “keratoconus free” before doing such an operation, otherwise he will be rasping a cornea which is already thin and has to be treated with operation of firming by linking it with extra fibres to enhance the corneal tissue. The proposed approach helps making this fatal decision

with such a high starting accuracy. Based upon this novel and straightforward algorithm new approaches can be invented to reach higher accuracies and more precise decision.

# PUBLICATIONS

[1] Sarah Ali Hasan, Mandeep Singh "An Algorithm to differentiate Astigmatism from Keratoconus in Axial Topographic images", BEATS-2014 International Conference, (Published on 14-15 Feb).

[2] Sarah Ali Hasan, Dr. Mandeep Singh, "Automatic Diagnosis of Astigmatism for Pentacam Sagittal Maps", Third International Workshop on Recent Advances in Medical Informatics (RAMI-2014) (Accepted to be published on (27-29Sep).

# REFRENCES


[1] Amar Agarwal , Athiya Agarwal ,& Soosan *Jacob* "Dr. Agarwal's Textbook on Corneal Topography Including Pentacam and Anterior Segment Oct", second edition, ( 2010).

[2] T.Reinhard, Essentials In Ophthalmology: "Cornea and External Eye Disease" D. F. P. Larkin (Eds.)

[3] Kara Rogers. "The Human Body-The Eye; The physiology of human perception", Encyclopædia Britannica, Inc. Britannica,( 2011).

[4] Michael Goggin, Astigmatism – Optics, Physiology and Management, InTech, Janeza Trdine 9, 51000 Rijeka, Croatia, (2012) InTech .

[5] *Melanie C. Corbett,* Corneal topography Basic principles and applications to refractive srgery, (2000); (www.optometry.co.uk).

[6] Maolong Tang, Raj Shekhar*, and David Huang "Mean Curvature Mapping for Detection of Corneal Shape Abnormality". IEEE transactions on medical imaging, vol. 24, no. 3, (2005).

[7] Ke Yao, Xiajing Tang, Panpan Ye, "Corneal Astigmatism, High Order Aberrations, and Optical Quality After Cataract Surgery: Microincision Versus Small Incision", Journal of Refractive Surgery Volume 22, (2006).

[8] Keith Croes Reprintd "The Alpins Method: A Breakthrough in Astigmatism Analysis", MEDICAL ELECTRONICS, (1998).

[9] Michael W. Belin, "Topography and Scheimpflug Imaging", Cataract & Refractive Surgery Today, January (2006)

[10] Michael W. Belin, "Keratoconus Detection with the Oculus Pentacam Enhanced Display" Highlights of Ophthalmology, volume 35, number 6.

[11] Damien Gatinel, Jacques Malet, Thanh Hoang-Xuan, and Dimitri T. Azar, "Corneal Elevation Topography: Best Fit Sphere, Elevation Distance, Asphericity, Toricity, and Clinical Implications" , (2010).

[12] Rajeev jain and SPS Grewal, "Pentacam: Principle and Clinical Applications", Journal Of Current Glaucoma Practice, (2009)

[13]. Rajeev Jain, Grewal "Pentacam: Principle and clinical applications", eye institute, Chandigarh, India. Journal of current Glaucoma Practice, 3(2):20-32, (2009);

[14] Ye Han, "A Mathematic model to correct myopic astigmatism" (2010) IEEE

[15] Liliane Ventura Andr Mhcio Vieira Messias Sidney J. Faria e Sousa "Automatic Measurements of the Radius of Curvature of the Cornea in Slit Lamp" , 22nd Annual EMBS International Conference, (2000), Chicago IL.

[16] Michael D. Twa, Srinivasan Parthasarathy, Cynthia Roberts "Automated Decision Tree Classification of Corneal Shape", (2010).

[17] Jack T. Holladay, "Keratoconus Detection Using Corneal Topography", Presented at the NIDEK NAVEX Seminar, World Congress of Ophthalmology; (2008); Hong Kong, China. Also available at ( journalofrefractivesurgery.com).

[18] Keith Marsolo, Michael Twa, Mark A. Bullimore, and Srinivasan Parthasarathy "Spatial Modeling and Classification of Corneal Shape"

[19] Qin Li, Jinghua Wang, Jane You "Refractive Error Detection via Group Sparse Representation" , (2010) IEEE.

[20] Weaam Alkhaldi, D. Robert Iskande ,"Enhancing the Standard Operating Range of a Placido Disk Videokeratoscope for Corneal Surface Estimation" IEEE transactions on biomedical engineering, (2009).

[21] David Alonso-Caneiro, D. Robert Iskander, and Michael J. Collin "Computationally Efficient Interference Detection in Video keratoscopy Images", (2008) IEEE

[22] Jay H Kashmir, Mark J Mannis, and Edward J Holland, “Cornea”, 3rd edition , Elsevier (2011).

[23] James S. W., Miguel R.J., Jacinto S.R, "Keratoconus: A review", Contact Lens and Anterior Eye, Volume 33, Issue 4, pp.157–166, (2010).

[24] Michael w. Belin, jack t. Holladay,j. Trevor Woodhams, & Iqbal k. Ahmed “The Pentacam: Precision, Confidence, Results, And Accurate “Ks!” ”, Cataract & Refractive surgery today, (2007).

[25]Refractive Power / Corneal Analyzer OPD-Scan III, *OPERATOR’S MANUAL US Edition,* By NIDEK CO., LTD., February (2011), 32186-P922A ,Printed in Japan.

[26]. Cynthia J. Roberts and Benno J. Züger “The Advantage and Principle of Dual Scheimpflug Imaging for Analyzing the Anterior Segment of the Human Eye”, Roberts/ Züger GALILEI Scheimpflug Analyzer 10.4.2006.

[27] Jack T. Holladay “Keratoconus Detection Using Corneal Topography”, Journal of Refractive Surgery Volume 25 October (Suppl) 2009.

[28] Naoyuki Maeda, Stephen D. Klyce, and Michael K. Smolek “Neural Network Classification of Corneal Topography”, Ophthalmology & Visual Science, Vol. 36, No. 7, (1995).

[29] T. Mihashi, Y. Hirohara, N. Maeda& T. Fujikado “Aberration Structure of Normal, Keratoconic, and Cataractous Eyes”, IEEE/ICME, International Conference on Complex Medical Engineering ,(2007).

[30] *Sahar Hemeda Elsayed,* Recent Trends in Diagnosis of Keratoconus, Faculty of Medicine Zagazig University, (2009).

[31] *Cynthia Roberts*, “The Accuracy of Tower Maps to Display Curvature Data in Corneal Topography Systems”, Investigative Ophthalmology & Visual Science, Vol. 35, No. 9, (1994)

[32] Fatemeh Toutounchian, Jamshid Shanbehzadeh, Mehdi Khanlari, “Detection of Keratoconus and Suspect Keratoconus by Machine Vision”, Proceedings of the International MultiConference of Engineering and Computer Scientists 2012 Vol I, IMECS 2012, March 14-16, (2012), Hong Cong.

[33] Keith Marsolo, Michael Twa, Mark A. Bullimore, and Srinivasan Parthasarathy, "Spatial Modeling and Classification of Corneal Shape", IEEE Transactions on Information Technology in Biomedicine, vol. 11, no. 2,( 2007)

[34] Qin Li, Jinghua Wang, Jane You, Bob Zhang, Fakhri Karray, "Refractive Error Detection via Group Sparse Representation", IEEE, (2010)

[35] "Pentacam A new look in the eye", A Special print behalf OCULUS Optikgeräte GmbH. Augenlicht, ( 2005). Available at: http://www.augenlicht.de

[36] Available at www.wikipedia.org

[37] Available at www.innovamed.com/Automated-Testing/Autorefractors/NIDEK-OPD-SCAN-III

[38] Available at www.medscape.com

[39] Available at www.pentacam.com

[40] Available at http://cms.revoptom.com

[41] Available at http://www.lasikguider.com

[42] Available at http://www.antelopemalloptometry.com/learn-about-astigmatism-and-astigmatic-refractive-error.php

[43] A.G. Lalkhen, A. McCluskey, "Clinical tests: sensitivity and specificity", Continuing Education Anesthesia, Critical Care & Pain, vol. 8 no. 6, pp. 221-223, (2008).